IOP PUBLISHING NONLINEARITY

Nonlinearity **25** (2012) 3423–3451 doi:10.1088/0951-7715/25/12/3423

Multi-site breathers in Klein–Gordon lattices: stability, resonances and bifurcations

Dmitry Pelinovsky and Anton Sakovich

Department of Mathematics, McMaster University, Hamilton ON L8S 4K1, Canada

Received 5 June 2012, in final form 9 October 2012
Published 2 November 2012
Online at stacks.iop.org/Non/25/3423

Recommended by R de la Llave

Abstract

We prove a general criterion of spectral stability of multi-site breathers in the discrete Klein–Gordon equation with a small coupling constant. In the anti-continuum limit, multi-site breathers represent excited oscillations at different sites of the lattice separated by a number of 'holes' (sites at rest). The criterion describes how the stability or instability of a multi-site breather depends on the phase difference and distance between the excited oscillators. Previously, only multi-site breathers with adjacent excited sites were considered within the first-order perturbation theory. We show that the stability of multi-site breathers with one-site holes changes for large-amplitude oscillations in soft nonlinear potentials. We also discover and study a symmetry-breaking (pitchfork) bifurcation of one-site and multi-site breathers in soft quartic potentials near the points of 1 : 3 resonance.

Mathematics Subject Classification: 37K60, 70K30, 70K42, 70K50

(Some figures may appear in colour only in the online journal)

1. Introduction

Space-localized and time-periodic breathers in nonlinear Hamiltonian lattices have been studied extensively in the past 20 years. These breathers model the oscillatory dynamics of particles due to the external forces and the interaction with other particles. A particularly simple model is the Klein–Gordon lattice, which is expressed by the discrete Klein–Gordon equation,

$$\ddot{u}_n + V'(u_n) = \epsilon(u_{n+1} - 2u_n + u_{n-1}), \qquad n \in \mathbb{Z}, \tag{1}$$

where $t \in \mathbb{R}$ is the evolution time, $u_n(t) \in \mathbb{R}$ is the displacement of the nth particle, $V : \mathbb{R} \to \mathbb{R}$ is a smooth on-site potential for the external forces, and $\epsilon \in \mathbb{R}$ is the coupling constant of the linear interaction between neighboring particles. For the sake of clarity, we will assume that the

potential V is symmetric, but a generalization can be formulated for non-symmetric potentials V. We will also assume that $V'(u)$ can be expanded in the power series near $u = 0$ by

$$V'(u) = u \pm u^3 + \mathcal{O}(u^5) \qquad \text{as} \quad u \to 0. \tag{2}$$

The plus and minus signs are referred to as the hard and soft potentials, respectively.

A simplification of analysis of the Klein–Gordon lattice was proposed by MacKay and Aubry [14] in the anti-continuum limit of small coupling constant $\epsilon \to 0$. This limit inspired many researchers to study existence, stability and global dynamics of space-localized and time-periodic breathers [3]. Since all oscillators are uncoupled at $\epsilon = 0$, one can construct time-periodic breathers localized at different sites of the lattice. *Such time-periodic space-localized solutions supported on a finite number of lattice sites at the anti-continuum limit are called the multi-site breathers*. All these multi-site breathers are uniquely continued with respect to the (small) coupling constant ϵ if the period of oscillations at different lattice sites is identical and the oscillations are synchronized either in-phase or anti-phase.

Spectral stability of multi-site breathers, which are continued from the anti-continuum limit $\epsilon = 0$, was considered by Morgante *et al* [15] with the help of numerical computations. These numerical computations suggested that spectral stability of small-amplitude multi-site breathers in the discrete Klein–Gordon equation (1) is similar to the spectral stability of multi-site solitons in the discrete nonlinear Schrödinger (DNLS) equation.

The DNLS approximation for small-amplitude and slowly varying oscillations relies on the asymptotic solution,

$$u_n(t) = \epsilon^{1/2}\left[a_n(\epsilon t)\mathrm{e}^{\mathrm{i}t} + \bar{a}_n(\epsilon t)\mathrm{e}^{-\mathrm{i}t}\right] + \mathcal{O}_{l^\infty}(\epsilon^{3/2}), \tag{3}$$

where $\epsilon > 0$ is assumed to be small, $\tau = \epsilon t$ is the slow time, and $a_n(\tau) \in \mathbb{C}$ is an envelope amplitude of nearly harmonic oscillations with the linear frequency $\omega = 1$. Substitution of (3) to (1) yields the DNLS equation to the leading order in ϵ,

$$2i\dot{a}_n = a_{n+1} - 2a_n + a_{n-1} \mp 3|a_n|^2 a_n, \qquad n \in \mathbb{Z}. \tag{4}$$

The hard and soft potentials (2) result in the defocusing and focusing cubic nonlinearities of the DNLS equation (4), respectively. Existence and continuous approximations of small-amplitude breathers in the discrete Klein–Gordon and DNLS equations were justified recently by Bambusi *et al* [4, 5]. The problem of bifurcation of small-amplitude breathers in Klein–Gordon lattices in connection to homoclinic bifurcations in the DNLS equations was also studied by James *et al* [9].

Multi-site solitons of the DNLS equation (4) can be constructed similarly to the multi-site breathers in the discrete Klein–Gordon equation (1). The time-periodic solutions are given by $a_n(\tau) = A_n\mathrm{e}^{-\mathrm{i}\omega\tau}$, where $\omega \in \mathbb{R}$ is a frequency of oscillations and $\{A_n\}_{n\in\mathbb{Z}}$ is a real-valued sequence of amplitudes decaying at infinity as $|n| \to \infty$. In the anti-continuum limit (which corresponds here to the limit $|\omega| \to \infty$ [16]), the multi-site solitons are supported on a finite number of lattice sites. The oscillations are in-phase or anti-phase, depending on the sign difference between the amplitudes $\{A_n\}_{n\in\mathbb{Z}}$ on the excited sites of the lattice.

Numerical results of [15] can be summarized as follows. *In the case of the focusing nonlinearity, the only stable multi-site solitons of the DNLS equation (4) near the anti-continuum limit correspond to the anti-phase oscillations on the excited sites of the lattice.* This conclusion does not depend on the number of 'holes' (oscillators at rest) between the excited sites at the anti-continuum limit. The stable oscillations in the case of the defocusing nonlinearity can be recovered from the stable anti-phase oscillations in the focusing case using the staggering transformation,

$$a_n(\tau) = (-1)^n \bar{b}_n(\tau)\mathrm{e}^{2\mathrm{i}\tau}, \tag{5}$$

which changes the DNLS equation (4) to the form,

$$2i\dot{b}_n = b_{n+1} - 2b_n + b_{n-1} \pm 3|b_n|^2 b_n, \qquad n \in \mathbb{Z}. \tag{6}$$

Consequently, we have the following statement. *In the case of the defocusing nonlinearity, the only stable multi-site solitons of the DNLS equation (4) with adjacent excited sites near the anti-continuum limit correspond to the in-phase oscillations on the excited sites of the lattice.*

The numerical observations of [15] were rigorously proved for the DNLS equation (4) by Pelinovsky *et al* [17]. Further details on the spectrum of a linearized operator associated with the multi-site solitons near the anti-continuum limit of the DNLS equation are obtained in our previous work [18].

Similar conclusions on the spectral stability of breathers in the discrete Klein–Gordon equation (1) were reported in the literature under some simplifying assumptions. Archilla *et al* [2] used the perturbation theory for spectral bands to consider two-site, three-site, and generally multi-site breathers. Theorem 6 in [2] states that *in-phase multi-site breathers are stable for hard potentials and anti-phase breathers are stable for soft potentials for* $\epsilon > 0$. The statement of this result misses however that the corresponding computations are justified for multi-site breathers with adjacent excited sites: no 'holes' (oscillators at rest) in the limiting configuration at $\epsilon = 0$ are allowed. More recently, Koukouloyannis and Kevrekidis [12] recovered exactly the same conclusion using the averaging theory for Hamiltonian systems in action-angle variables developed earlier by MacKay *et al* [1, 13]. To justify the use of the first-order perturbation theory, the multi-site breathers were considered to have adjacent excited sites and no holes. The equivalence between these two approaches was addressed by Cuevas *et al* [8].

It is the goal of our paper to rigorously prove the stability criterion for all multi-site breathers, including breathers with holes between excited sites in the anti-continuum limit. We will use perturbative arguments for characteristic exponents of the Floquet monodromy matrices. To be able to work with the higher-order perturbation theory, we will combine these perturbative arguments with the theory of tail-to-tail interactions of individual breathers in lattice differential equations. Although the tail-to-tail interaction theory is well-known for continuous partial differential equations [20], it is the first time to our knowledge when this theory is extended to nonlinear lattices.

Multi-site breathers with holes have been recently considered by Yoshimura [25] in the context of the diatomic Fermi–Pasta–Ulam lattice near the anti-continuum limit. In order to separate variables n and t and to perform computations using the discrete Sturm theorem (similar to the one used in the context of NLS lattices in [17]), the interaction potential was assumed to be nearly homogeneous of degree four and higher. Similar work was performed for the Klein–Gordon lattices with a purely anharmonic interaction potential [26]. Compared to this work, our treatment is valid for a non-homogeneous on-site potential V satisfying expansion (2) and for the quadratic interaction potential.

Within our work, we have discovered new important details on the spectral stability of multi-site breathers, which were missed in the previous works [2, 12, 15]. In the case of soft potentials, breathers of the discrete Klein–Gordon equation (1) cannot be continued far away from the small-amplitude limit described by the DNLS equation (4) because of the resonances between the nonlinear oscillators at the excited sites and the linear oscillators at the sites at rest. Branches of breather solutions continued from the anti-continuum limit above and below the resonance are disconnected. In addition, these resonances change the stability conclusion. In particular, the anti-phase oscillations may become unstable in soft nonlinear potentials even if the coupling constant is sufficiently small.

Another interesting feature of soft potentials is the symmetry-breaking (pitchfork) bifurcation of one-site and multi-site breathers that occur near the point of resonances. In symmetric potentials, the first non-trivial resonance occurs at 1 : 3 resonance. We analyse this bifurcation by using asymptotic expansions and reduction of the discrete Klein–Gordon equation (1) to a normal form, which coincides with the nonlinear Duffing oscillator perturbed by a small harmonic forcing. It is interesting that the normal form equation for 1 : 3 resonance which we analyse here is different from the normal form equations considered in the previous studies of 1 : 3 resonance [7, 21, 22]. The difference is explained by the fact that we are looking at bifurcations of periodic solutions far from the equilibrium points, whereas the standard normal form equations for 1 : 3 resonance are derived in a neighborhood of equilibrium points. Note that an analytical study of bifurcations of small breather solutions close to a point of 1 : 3 resonance for a diatomic Fermi–Pasta–Ulam lattice was performed by James and Kastner [10].

The paper is organized as follows. Existence of space-localized and time-periodic breathers near the anti-continuum limit is reviewed in section 2. Besides the persistence results based on the implicit function arguments as in [14], we also develop a new version of the tail-to-tail interaction theory for multi-site breathers in the discrete Klein–Gordon equation (1). The main result on spectral stability of multi-site breathers for small coupling constants is formulated and proved in section 3. Section 4 illustrates the existence and spectral stability of multi-site breathers in soft potentials numerically. Section 5 is devoted to studies of the symmetry-breaking (pitchfork) bifurcation using asymptotic expansions and normal forms for 1 : 3 resonance. Section 6 summarizes our findings. The appendix compares Floquet theory with the spectral band theory and Hamiltonian averaging to show equivalence of our conclusions with those reported earlier in [2, 12].

2. Existence of multi-site breathers near the anti-continuum limit

In what follows, we will use bold-faced notations for vectors in discrete space $l^p(\mathbb{Z})$ defined by their norms

$$\|\boldsymbol{u}\|_{l^p} := \left(\sum_{n\in\mathbb{Z}} |u_n|^p\right)^{1/p}, \qquad p \geqslant 1.$$

Components of $\boldsymbol{u}$ are denoted by u_n for $n \in \mathbb{Z}$. These components can be functions of t, in which case they are considered in Hilbert–Sobolev spaces $H^s_{\rm per}(0, T)$ of T-periodic functions equipped with the norm,

$$\|f\|_{H^s_{\rm per}} := \left(\sum_{m\in\mathbb{Z}} (1+m^2)^s |c_m|^2\right)^{1/2}, \qquad s \geqslant 0,$$

where the set of coefficients $\{c_m\}_{m\in\mathbb{Z}}$ defines the Fourier series of a T-periodic function f,

$$f(t) = \sum_{m\in\mathbb{Z}} c_m \exp\left(\frac{2\pi i m t}{T}\right), \qquad t \in [0, T].$$

We consider space-localized and time-periodic breathers $\boldsymbol{u} \in l^2(\mathbb{Z}, H^2_{\rm per}(0, T))$ of the discrete Klein–Gordon equation (1) with smooth even V and $\epsilon > 0$. Parameter $T > 0$ represents the fundamental period of the time-periodic breathers. Accounting for symmetries, we shall work in the restriction of $H^s_{\rm per}(0, T)$ to the space of even T-periodic functions,

$$H^s_e(0, T) = \left\{ f \in H^s_{\rm per}(0, T) : \quad f(-t) = f(t), \quad t \in \mathbb{R} \right\}, \qquad s \geqslant 0.$$

At $\epsilon = 0$, we have an arbitrary family of multi-site breathers,

$$\boldsymbol{u}^{(0)}(t) = \sum_{k \in S} \sigma_k \varphi(t) \boldsymbol{e}_k, \tag{7}$$

where $\boldsymbol{e}_k$ is the unit vector in $l^2(\mathbb{Z})$, $S \subset \mathbb{Z}$ is a finite set of excited sites of the lattice, $\sigma_k \in \{+1, -1\}$ encodes the phase factor of the kth oscillator, and $\varphi \in H^2_{\rm per}(0, T)$ is an even solution of the nonlinear oscillator equation at the energy level E,

$$\ddot{\varphi} + V'(\varphi) = 0 \quad \Rightarrow \qquad E = \frac{1}{2}\dot{\varphi}^2 + V(\varphi). \tag{8}$$

The unique even solution $\varphi(t)$ satisfies the initial condition,

$$\varphi(0) = a, \qquad \dot{\varphi}(0) = 0, \tag{9}$$

where a is the smallest positive root of $V(a) = E$ for a fixed value of E. Period of oscillations T is uniquely defined by the energy level E,

$$T = \sqrt{2} \int_{-a}^{a} \frac{{\rm d}\varphi}{\sqrt{E - V(\varphi)}}. \tag{10}$$

Because $\varphi(t)$ is T-periodic, we have

$$\partial_E \varphi(T) = a'(E) = \frac{1}{V'(a)}, \tag{11}$$

$$\partial_E \dot{\varphi}(T) = -\ddot{\varphi}(T) T'(E) = V'(a) T'(E). \tag{12}$$

Our main example of the nonlinear potential V is the truncation of the expansion (2) at the first two terms:

$$V'(u) = u \pm u^3. \tag{13}$$

The dependence T versus E is computed numerically from (10) and is shown in figure 1 together with the phase portraits of the system (8). For the hard potential with the plus sign, the period T is a decreasing function of E in $(0, 2\pi)$, whereas for the soft potential with the minus sign, the period T is an increasing function of E with $T > 2\pi$.

Remark 1. All nonlinear oscillators at the excited sites of $S \subset \mathbb{Z}$ in the limiting configuration (7) have the same period T. Two oscillators at the jth and kth sites are said to be in-phase if $\sigma_j \sigma_k = 1$ and anti-phase if $\sigma_j \sigma_k = -1$.

Persistence of the limiting configuration (7) as a space-localized and time-periodic breather of the discrete Klein–Gordon equation (1) for small values of ϵ is established by MacKay and Aubry [14]. The following theorem gives the relevant details of the theory that are useful in our analysis.

Theorem 1. *Fix the period T and the solution $\varphi \in H^2_e(0, T)$ of the nonlinear oscillator equation (8) with an even $V \in C^\infty(\mathbb{R})$ satisfying (2) and assume that $T \neq 2\pi n$, $n \in \mathbb{N}$ and $T'(E) \neq 0$. Define $\boldsymbol{u}^{(0)}$ by the representation (7) with fixed $S \subset \mathbb{Z}$ and $\{\sigma_k\}_{k \in S}$. There are $\epsilon_0 > 0$ and $C > 0$ such that for all $\epsilon \in (-\epsilon_0, \epsilon_0)$, there exists a unique solution $\boldsymbol{u}^{(\epsilon)} \in l^2(\mathbb{Z}, H^2_e(0, T))$ of the discrete Klein–Gordon equation (1) satisfying*

$$\| \boldsymbol{u}^{(\epsilon)} - \boldsymbol{u}^{(0)} \|_{l^2(\mathbb{Z}, H^2_{\rm per}(0,T))} \leqslant C|\epsilon|. \tag{14}$$

Moreover, the map $\mathbb{R} \ni \epsilon \mapsto \boldsymbol{u}^{(\epsilon)} \in l^2(\mathbb{Z}, H^2_e(0, T))$ is C^∞ for all $\epsilon \in (-\epsilon_0, \epsilon_0)$.

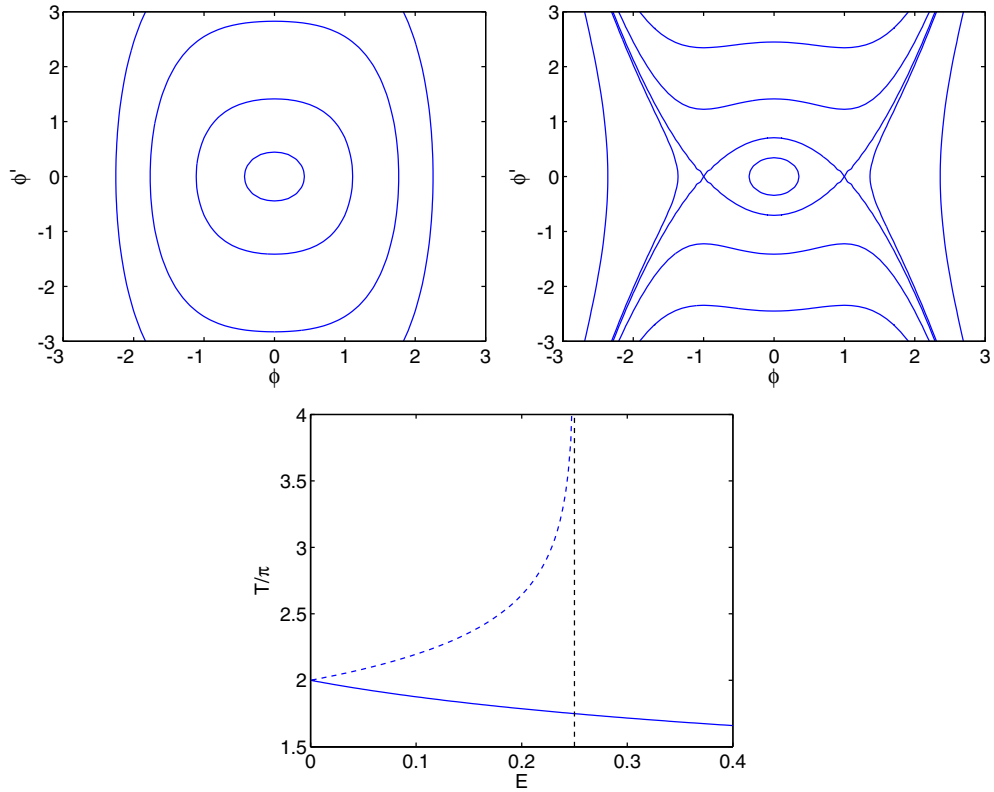

Figure 1. Top: the phase plane $(\varphi, \dot{\varphi})$ for the hard (left) and soft (right) potentials (13). Bottom: the period T versus energy E for the hard (solid) and soft (dashed) potentials.

Proof. Thanks to the translational invariance of the nonlinear oscillator equation (8), we fix an even φ according to the initial condition (9) and consider $H_e^s(0, T)$, the restriction of $H_{\rm per}^s(0, T)$ to even functions. Under the condition $T'(E) \neq 0$, operator

$$L_e = \partial_t^2 + V''(\varphi(t)) : H_e^2(0, T) \to L_e^2(0, T)$$

is invertible, because the only eigenvector $\dot{\varphi}$ of $L = \partial_t^2 + V''(\varphi(t)) : H_{\rm per}^2(0, T) \to L_{\rm per}^2(0, T)$ is odd in t. Similarly, operator

$$L_0 = \partial_t^2 + 1 : H_{\rm per}^2(0, T) \to L_{\rm per}^2(0, T)$$

is invertible if $T \neq 2\pi n$, $n \in \mathbb{N}$.

Substituting $\boldsymbol{u} = \boldsymbol{u}^{(0)} + \boldsymbol{w}$, where $\boldsymbol{u}^{(0)}$ is the limiting breather (7) to the discrete Klein–Gordon equation (1), we obtain the coupled system of differential–difference equations

$$L_e w_n = \epsilon(u_{n+1}^{(0)} - 2u_n^{(0)} + u_{n-1}^{(0)}) + N_n(\boldsymbol{w}, \epsilon), \qquad n \in S \tag{15}$$

and

$$L_0 w_n = \epsilon(u_{n+1}^{(0)} - 2u_n^{(0)} + u_{n-1}^{(0)}) + N_n(\boldsymbol{w}, \epsilon), \qquad n \in \mathbb{Z}\backslash S, \tag{16}$$

where

$$N_n(\boldsymbol{w}, \epsilon) = \epsilon(w_{n+1} - 2w_n + w_{n-1}) + Q_n(w_n)$$

and

$$Q_n(w_n) = V'(u_n^{(0)}) + V''(u_n^{(0)})w_n - V'(u_n^{(0)} + w_n).$$

Since $V \in C^\infty(\mathbb{R})$, the nonlinear function $Q_n(w_n)$ is C^∞ for all $w_n \in \mathbb{R}$. Because the discrete Laplacian is a bounded operator from $l^2(\mathbb{Z})$ to $l^2(\mathbb{Z})$ and $H^2_{\rm per}(0,T)$ forms a Banach algebra with respect to pointwise multiplication, we conclude that the vector field $\boldsymbol{N}(\boldsymbol{w},\epsilon) : l^2(\mathbb{Z}, H^2_{\rm per}(0,T)) \times \mathbb{R} \to l^2(\mathbb{Z}, H^2_{\rm per}(0,T))$ is a C^∞ map. Moreover, for any $\boldsymbol{w}$ in a ball in $l^2(\mathbb{Z}, H^2_{\rm per}(0,T))$ centred at 0 with radius $\delta > 0$, there are constants $C_\delta, D_\delta > 0$ such that

$$\|\boldsymbol{N}(\boldsymbol{w},\epsilon)\|_{l^2(\mathbb{Z},H^2_{\rm per}(0,T))} \leqslant C_\delta \left(\epsilon\|\boldsymbol{w}\|_{l^2(\mathbb{Z},H^2_{\rm per}(0,T))} + \|\boldsymbol{w}\|^2_{l^2(\mathbb{Z},H^2_{\rm per}(0,T))}\right)$$

and

$$\|\boldsymbol{N}(\boldsymbol{w}_1,\epsilon) - \boldsymbol{N}(\boldsymbol{w}_2,\epsilon)\|_{l^2(\mathbb{Z},H^2_{\rm per}(0,T))} \leqslant D_\delta \left(\epsilon + \|\boldsymbol{w}_1\|_{l^2(\mathbb{Z},H^2_{\rm per}(0,T))} + \|\boldsymbol{w}_2\|_{l^2(\mathbb{Z},H^2_{\rm per}(0,T))}\right) \times \|\boldsymbol{w}_1 - \boldsymbol{w}_2\|_{l^2(\mathbb{Z},H^2_{\rm per}(0,T))}.$$

Thanks to the invertibility of the linearized operators L_e and L_0 on L^2_e, the result of the theorem follows from the implicit function theorem (theorem 4.E in [27]) and the map $\mathbb{R} \ni \epsilon \mapsto \boldsymbol{u}^{(\epsilon)} \in l^2(\mathbb{Z}, H^2_e(0,T))$ is C^∞ for all small ϵ. □

Remark 2. Although persistence of other breather configurations, where oscillators are neither in-phase nor anti-phase, can not be *a priori* excluded, we restrict our studies to the most important and physically relevant breather configurations covered by theorem 1.

We shall now introduce the concept of the fundamental breather for the set $S = \{0\}$. Multi-site breathers for small $\epsilon > 0$ can be approximated by the superposition of fundamental breathers at a generic set S of excited sites up to and including the order, at which the tail-to-tail interactions of these breathers occur.

Definition 1. *Let $\boldsymbol{u}^{(\epsilon)} \in l^2(\mathbb{Z}, H^2_e(0,T))$ be the solution of the discrete Klein–Gordon equation (1) for small $\epsilon > 0$ defined by theorem 1 for a given $\boldsymbol{u}^{(0)}(t) = \varphi(t)\boldsymbol{e}_0$. This solution is called the fundamental breather and we denote it by $\phi^{(\epsilon)}$.*

By theorem 1, we can use the Taylor series expansion,

$$\phi^{(\epsilon)} = \phi^{(\epsilon,N)} + \mathcal{O}_{l^2(\mathbb{Z},H^2_{\rm per}(0,T))}(\epsilon^{N+1}), \qquad \phi^{(\epsilon,N)} = \sum_{k=0}^{N} \frac{\epsilon^k}{k!}\frac{d^k}{d\epsilon^k}\phi^{(\epsilon)}\bigg|_{\epsilon=0}, \tag{17}$$

up to any integer $N \geqslant 0$. Thanks to the discrete translational invariance of the lattice, the fundamental breather can be centred at any site $j \in \mathbb{Z}$. Let $\tau_j : l^2(\mathbb{Z}) \to l^2(\mathbb{Z})$ be the shift operator defined by

$$(\tau_j \boldsymbol{u})_n = u_{n-j}, \qquad n \in \mathbb{Z}.$$

If $\phi^{(\epsilon)}$ is centred at site 0, then $\tau_j\phi^{(\epsilon)}$ is centred at site $j \in \mathbb{Z}$. The simplest multi-site breather is given by the two excited nodes at $j \in \mathbb{Z}$ and $k \in \mathbb{Z}$ with $j \neq k$.

Lemma 1. *Let $\boldsymbol{u}^{(0)}(t) = \sigma_j\varphi(t)\boldsymbol{e}_j + \sigma_k\varphi(t)\boldsymbol{e}_k$ with $j \neq k$ and $N = |j-k| \geqslant 1$. Let $\boldsymbol{u}^{(\epsilon)} \in l^2(\mathbb{Z}, H^2_e(0,T))$ be the corresponding solution of the discrete Klein–Gordon equation (1) for small $\epsilon > 0$ defined by theorem 1. Let $\{\varphi_m\}_{m=1}^N \in H^2_e(0,T)$ be defined recursively by*

$$L_0\varphi_m := (\partial_t^2 + 1)\varphi_m = \varphi_{m-1}, \qquad m = 1, 2, \ldots, N, \tag{18}$$

starting with $\varphi_0 = \varphi$, and let $\psi_N \in H^2_e(0,T)$ be defined by

$$L_e \psi_N := (\partial_t^2 + V''(\varphi(t)))\psi_N = \varphi_{N-1}. \tag{19}$$

Then, we have

$$\boldsymbol{u}^{(\epsilon)} = \sigma_j \tau_j \boldsymbol{\phi}^{(\epsilon,N)} + \sigma_k \tau_k \boldsymbol{\phi}^{(\epsilon,N)} + \epsilon^N \left(\sigma_j \boldsymbol{e}_k + \sigma_k \boldsymbol{e}_j\right)(\psi_N - \varphi_N) + \mathcal{O}_{l^2(\mathbb{Z}, H^2_{\rm per}(0,T))}(\epsilon^{N+1}). \tag{20}$$

Proof. By theorem 1, the limiting configuration $\boldsymbol{u}^{(0)}(t) = \sigma_j \varphi(t) \boldsymbol{e}_j + \sigma_k \varphi(t) \boldsymbol{e}_k$ with two excited sites generates a C^∞ map, which can be expanded up to the $N+1$-order,

$$\boldsymbol{u}^{(\epsilon)} = \sum_{k=0}^{N} \frac{\epsilon^k}{k!} \frac{d^k}{d\epsilon^k} \boldsymbol{u}^{(\epsilon)} \Big|_{\epsilon=0} + \mathcal{O}_{l^2(\mathbb{Z}, H^2_{\rm per}(0,T))}(\epsilon^{N+1}). \tag{21}$$

Substituting (21) into (1) generates a sequence of equations at each order of ϵ, which we consider up to and including the terms of order N.

The central excited site at $n = 0$ in the fundamental breather $\boldsymbol{\phi}^{(\epsilon)}$ generates fluxes, which reach sites $n = \pm m$ at the m-th order. Because $\boldsymbol{\phi}^{(\epsilon,m)}$ is compactly supported on $\{-m, -m+1, ..., m\}$ and all sites with $n \neq 0$ contain no oscillations at the 0th order, we have

$$\phi^{(\epsilon,m)}_{\pm m} = \epsilon^m \varphi_m, \tag{22}$$

where $\{\varphi_m\}_{m=1}^N \in H^2_e(0,T)$ are computed from the linear inhomogeneous equations (18) starting with $\varphi_0 = \varphi$. Note that equations (18) are uniquely solvable because $T \neq 2\pi n$, $n \in \mathbb{N}$.

For definiteness, let us assume that $j = 0$ and $k = N \geqslant 1$. The fluxes from the excited sites $n = 0$ and $n = N$ meet at the $N/2$th order at the middle site $n = N/2$ if N is even or they overlap at the $(N+1)/2$th order at the two sites $n = (N-1)/2$ and $n = (N+1)/2$ if N is odd. In either case, because of the expansion (2), the nonlinear superposition of these fluxes affects terms at the order $3N/2$th or $3(N+1)/2$th orders, that is, beyond the N-th order of the expansion (20). Therefore, the nonlinear superposition of fluxes in higher orders of ϵ will definitely be beyond the N-th order of the expansion (20).

Up to the Nth order, all correction terms are combined together as a sum of correction terms from the decomposition (17) centred at the jth and kth sites, that is, we have

$$\boldsymbol{u}(\epsilon) = \sigma_j \tau_j \boldsymbol{\phi}^{(\epsilon,N-1)}(\epsilon) + \sigma_k \tau_k \boldsymbol{\phi}^{(\epsilon,N-1)}(\epsilon) + \mathcal{O}_{l^2(\mathbb{Z}, H^2_{\rm per}(0,T))}(\epsilon^N). \tag{23}$$

At the Nth order, the flux from jth site arrives to the kth site and vice versa. Therefore, besides the Nth order correction terms from the decomposition (17), we have additional terms $\epsilon^N \left(\sigma_j \boldsymbol{e}_k + \sigma_k \boldsymbol{e}_j\right) \psi_N$ at the sites $n = j$ and $n = k$. Thanks to the linear superposition principle, these additional terms are given by solutions of the inhomogeneous equations (19), which are uniquely solvable in $H^2_e(0,T)$ because $T'(E) \neq 0$. We also have to subtract $\epsilon^N \left(\sigma_j \boldsymbol{e}_k + \sigma_k \boldsymbol{e}_j\right) \varphi_N$ from the Nth order of $\sigma_j \tau_j \boldsymbol{\phi}^{(\epsilon,N)} + \sigma_k \tau_k \boldsymbol{\phi}^{(\epsilon,N)}$, because these terms were computed under the assumption that the k-th site contained no oscillations at the order 0 for $\sigma_j \tau_j \boldsymbol{\phi}^{(\epsilon,N)}$ and vice versa. Combined all together, the expansion (20) is justified up to terms of the Nth order. □

3. Stability of multi-site breathers near the anti-continuum limit

Let $\boldsymbol{u} \in l^2(\mathbb{Z}, H^2_e(0,T))$ be a multi-site breather in theorem 1 and $\epsilon > 0$ be a small parameter of the discrete Klein–Gordon equation (1). When we study stability of breathers, we understand the spectral stability, which is associated with the linearization of the discrete Klein–Gordon equation (1) by using a perturbation $\boldsymbol{w}(t)$ in the decomposition $\boldsymbol{u}(t) + \boldsymbol{w}(t)$.

Neglecting quadratic and higher-order terms in $\boldsymbol{w}$, we obtain the linearized discrete Klein–Gordon equation,

$$\ddot{w}_n + V''(u_n)w_n = \epsilon(w_{n+1} - 2w_n + w_{n-1}), \qquad n \in \mathbb{Z}. \tag{24}$$

Because $\boldsymbol{u}(t+T) = \boldsymbol{u}(t)$, an infinite-dimensional analogue of the Floquet theorem applies and the Floquet monodromy matrix $\mathcal{M}$ is defined by $\boldsymbol{w}(T) = \mathcal{M}\boldsymbol{w}(0)$. We say that the breather is stable if all eigenvalues of $\mathcal{M}$, called Floquet multipliers, are located on the unit circle and it is unstable if there is at least one Floquet multiplier outside the unit disc. Because the linearized system (24) is Hamiltonian, Floquet multipliers come in pairs μ_1 and μ_2 with $\mu_1\mu_2 = 1$.

For $\epsilon = 0$, Floquet multipliers can be computed explicitly because $\mathcal{M}$ is decoupled into a diagonal combination of 2-by-2 matrices $\{M_n\}_{n\in\mathbb{Z}}$, which are computed from solutions of the linearized equations

$$\ddot{w}_n + w_n = 0, \qquad n \in \mathbb{Z}\backslash S \tag{25}$$

and

$$\ddot{w}_n + V''(\varphi)w_n = 0, \qquad n \in S. \tag{26}$$

The first problem (25) admits the exact solution,

$$w_n(t) = w_n(0)\cos(t) + \dot{w}_n(0)\sin(t) \Rightarrow M_n = \begin{bmatrix} \cos(T) & \sin(T) \\ -\sin(T) & \cos(T) \end{bmatrix}, \ n \in \mathbb{Z}\backslash S. \tag{27}$$

Each M_n for $n \in \mathbb{Z}\backslash S$ has two Floquet multipliers at $\mu_1 = \mathrm{e}^{\mathrm{i}T}$ and $\mu_2 = \mathrm{e}^{-\mathrm{i}T}$. If $T \neq 2\pi n$, $n \in \mathbb{N}$, the Floquet multipliers μ_1 and μ_2 are located on the unit circle bounded away from the point $\mu = 1$.

The second problem (26) also admits the exact solution,

$$w_n(t) = \frac{\dot{w}_n(0)}{\ddot{\varphi}(0)}\dot{\varphi}(t) + \frac{w_n(0)}{\partial_E\varphi(0)}\partial_E\varphi(t), \qquad n \in S, \tag{28}$$

where $\varphi(t)$ is a solution of the nonlinear oscillator equation (8) with the initial condition (9). Using identities (11) and (12), we obtain,

$$M_n = \begin{bmatrix} 1 & 0 \\ T'(E)[V'(a)]^2 & 1 \end{bmatrix}, \qquad n \in S.$$

Note that $V'(a) \neq 0$ (or T is infinite). If $T'(E) \neq 0$, each M_n for $n \in S$ has the Floquet multiplier $\mu = 1$ of geometric multiplicity one and algebraic multiplicity two.

We conclude that if $T \neq 2\pi n$, $n \in \mathbb{N}$ and $T'(E) \neq 0$, the limiting multi-site breather (7) at the anti-continuum limit $\epsilon = 0$ has an infinite number of semi-simple Floquet multipliers at $\mu_1 = \mathrm{e}^{\mathrm{i}T}$ and $\mu_2 = \mathrm{e}^{-\mathrm{i}T}$ bounded away from the Floquet multiplier $\mu = 1$ of algebraic multiplicity $2|S|$ and geometric multiplicity $|S|$.

Semi-simple multipliers on the unit circle are structurally stable in Hamiltonian dynamical systems (chapter III in [24]). Under perturbations in the Hamiltonian, Floquet multipliers of the same Krein signature do not move off the unit circle unless they coalesce with Floquet multipliers of the opposite Krein signature [6]. Therefore, the instability of the multi-site breather may only arise from the splitting of the Floquet multiplier $\mu = 1$ of algebraic multiplicity $2|S|$ for $\epsilon \neq 0$.

To consider Floquet multipliers, we can introduce the characteristic exponent λ in the decomposition $\boldsymbol{w}(t) = \boldsymbol{W}(t)\mathrm{e}^{\lambda t}$. If $\mu = \mathrm{e}^{\lambda T}$ is the Floquet multiplier of the monodromy operator $\mathcal{M}$, then $\boldsymbol{W} \in l^2(\mathbb{Z}, H^2_{\mathrm{per}}(0, T))$ is a solution of the eigenvalue problem,

$$\ddot{W}_n + V''(u_n)W_n + 2\lambda\dot{W}_n + \lambda^2 W_n = \epsilon(W_{n+1} - 2W_n + W_{n-1}), \quad n \in \mathbb{Z}. \tag{29}$$

In particular, Floquet multiplier $\mu = 1$ corresponds to the characteristic exponent $\lambda = 0$. The generalized eigenvector $\boldsymbol{Z} \in l^2(\mathbb{Z}, H^2_{\rm per}(0,T))$ of the eigenvalue problem (29) for $\lambda = 0$ solves the inhomogeneous problem,

$$\ddot{Z}_n + V''(u_n)Z_n = \epsilon(Z_{n+1} - 2Z_n + Z_{n-1}) - 2\dot{W}_n, \qquad n \in \mathbb{Z}, \tag{30}$$

where $\boldsymbol{W}$ is the eigenvector of (29) for $\lambda = 0$. To normalize $\boldsymbol{Z}$ uniquely, we add a constraint that $\boldsymbol{Z}$ is orthogonal to $\boldsymbol{W}$ with respect to the inner product

$$\langle \boldsymbol{W}, \boldsymbol{Z} \rangle_{l^2(\mathbb{Z}, L^2_{\rm per}(0,T))} := \sum_{n\in\mathbb{Z}} \int_0^T \bar{W}_n(t) Z_n(t)\, {\rm d}t.$$

At $\epsilon = 0$, the eigenvector $\boldsymbol{W}$ of the eigenvalue problem (29) for $\lambda = 0$ is spanned by the linear combination of $|S|$ fundamental solutions,

$$\boldsymbol{W}^{(0)}(t) = \sum_{k\in S} c_k \dot{\varphi}(t) \boldsymbol{e}_k. \tag{31}$$

The generalized eigenvector $\boldsymbol{Z}$ is spanned by the linear combination of $|S|$ solutions,

$$\boldsymbol{Z}^{(0)}(t) = -\sum_{k\in S} c_k v(t) \boldsymbol{e}_k, \qquad v := 2L_e^{-1}\ddot{\varphi}, \tag{32}$$

where $L_e = \partial_t^2 + V''(\varphi(t)) : H^2_e(0,T) \to L^2_e(0,T)$ is invertible and $\ddot{\varphi} \in L^2_e(0,T)$ (see the proof of theorem 1). Note that $\langle \dot{\varphi}, v \rangle_{L^2_{\rm per}(0,T)} = 0$ because $\dot{\varphi}$ is odd and v is even in t.

Because of the translational invariance in t, we note that if $\boldsymbol{u} = \boldsymbol{\phi}^{(\epsilon)}$ is the fundamental breather in Definition 1, then $\boldsymbol{W} = \partial_t \boldsymbol{\phi}^{(\epsilon)} \equiv \boldsymbol{\theta}^{(\epsilon)} \in l^2(\mathbb{Z}, H^2_{\rm per}(0,T))$ is the eigenvector of the eigenvalue problem (29) for $\lambda = 0$ and small $\epsilon > 0$ and there exists a generalized eigenvector $\boldsymbol{Z} \equiv \boldsymbol{\mu}^{(\epsilon)} \in l^2(\mathbb{Z}, H^2_{\rm per}(0,T))$ of the inhomogeneous problem (30), which exists because $\partial_t \boldsymbol{\theta}^{(\epsilon)}$ has the opposite parity in t compared to $\boldsymbol{\theta}^{(\epsilon)}$.

By Taylor series expansions (17), for any integer $N \geqslant 0$, we have

$$\boldsymbol{\theta}^{(\epsilon)} = \boldsymbol{\theta}^{(\epsilon,N)} + \mathcal{O}_{l^2(\mathbb{Z}, H^2_{\rm per}(0,T))}(\epsilon^{N+1}), \qquad \boldsymbol{\mu}^{(\epsilon)} = \boldsymbol{\mu}^{(\epsilon,N)} + \mathcal{O}_{l^2(\mathbb{Z}, H^2_{\rm per}(0,T))}(\epsilon^{N+1}), \tag{33}$$

where $\boldsymbol{\theta}^{(\epsilon,N)}$ and $\boldsymbol{\mu}^{(\epsilon,N)}$ are polynomials in ϵ of degree N. It follows from equations (31) and (32) that

$$\boldsymbol{\theta}^{(0)} = \dot{\varphi}(t)\boldsymbol{e}_0, \qquad \boldsymbol{\mu}^{(0)} = -v(t)\boldsymbol{e}_0. \tag{34}$$

This formalism sets up the scene for the perturbation theory, which is used to prove the main result on spectral stability of multi-site breathers. We start with a simple multi-site breather configuration with equal distances between excited sites and then upgrade this result to multi-site breathers with non-equal distances between excited sites.

Lemma 2. *Under assumptions of Theorem 1, let* $\boldsymbol{u}^{(0)}(t) = \sum_{j=1}^M \sigma_j \varphi(t) \boldsymbol{e}_{jN}$ *with fixed* $M, N \in \mathbb{N}$ *and* $\boldsymbol{u}^{(\epsilon)} \in l^2(\mathbb{Z}, H^2_e(0,T))$ *be the corresponding solution of the discrete Klein–Gordon equation (1) for small* $\epsilon > 0$ *defined by theorem 1. Let* $\{\varphi_m\}_{m=0}^N$ *be defined by lemma 1 starting with* $\varphi_0 = \varphi$. *Then the eigenvalue problem (29) for small* $\epsilon > 0$ *has* $2M$ *small eigenvalues,*

$$\lambda = \epsilon^{N/2}\Lambda + \mathcal{O}(\epsilon^{(N+1)/2}),$$

where Λ *is an eigenvalue of the matrix eigenvalue problem*

$$-\frac{T^2(E)}{T'(E)}\Lambda^2 \boldsymbol{c} = K_N \mathcal{S} \boldsymbol{c}, \qquad \boldsymbol{c} \in \mathbb{C}^M. \tag{35}$$

Here the numerical coefficient K_N is given by

$$K_N = \int_0^T \dot{\varphi}\dot{\varphi}_{N-1}\,\mathrm{d}t$$

and the matrix $\mathcal{S} \in \mathbb{M}^{M\times M}$ is given by

$$\mathcal{S} = \begin{bmatrix} -\sigma_1\sigma_2 & 1 & 0 & \dots & 0 & 0 \\ 1 & -\sigma_2(\sigma_1+\sigma_3) & 1 & \dots & 0 & 0 \\ 0 & 1 & -\sigma_3(\sigma_2+\sigma_4) & \dots & 0 & 0 \\ \vdots & \vdots & \vdots & \ddots & \vdots & \vdots \\ 0 & 0 & 0 & \dots & -\sigma_{M-1}(\sigma_{M-2}+\sigma_M) & 1 \\ 0 & 0 & 0 & \dots & 0 & -\sigma_M\sigma_{M-1} \end{bmatrix}.$$

Proof. At $\epsilon = 0$, the eigenvalue problem (29) admits eigenvalue $\lambda = 0$ of geometric multiplicity M and algebraic multiplicity $2M$, which is isolated from the rest of the spectrum. Perturbation theory in ϵ applies thanks to the smoothness of $\boldsymbol{u}^{(\epsilon)}$ in ϵ and V' in u. Perturbation expansions (so-called Puiseux series, see chapter 2 in [11] and recent work [23]) are smooth in powers of $\epsilon^{1/2}$ thanks to the Jordan block decomposition at $\epsilon = 0$.

We need to find out how the eigenvalue $\lambda = 0$ of algebraic multiplicity $2M$ split for small $\epsilon > 0$. Therefore, we are looking for the eigenvectors of the eigenvalue problem (29) in the subspace associated with the eigenvalue $\lambda = 0$ using the substitution $\lambda = \epsilon^{N/2}\tilde{\lambda}$ and the decomposition

$$\boldsymbol{W} = \sum_{j=1}^{M} c_j \left(\tau_{jN}\boldsymbol{\theta}^{(\epsilon,N)} - \epsilon^N(\boldsymbol{e}_{(j-1)N} + \boldsymbol{e}_{(j+1)N})\dot{\varphi}_N\right) + \epsilon^{N/2}\tilde{\lambda}\sum_{j=1}^{M} c_j\tau_{jN}\boldsymbol{\mu}^{(\epsilon,N_*)} + \epsilon^N\tilde{\boldsymbol{W}}, \quad (36)$$

where $N_* = N/2$ if N is even and $N_* = (N-1)/2$ if N is odd, whereas $\tilde{\boldsymbol{W}}$ is the remainder term at the N-th order in ϵ. The decomposition formula (36) follows from the superposition (20) up to the Nth order in ϵ. The terms $\epsilon^N\sum_{j=1}^{M} c_j(\boldsymbol{e}_{(j-1)N} + \boldsymbol{e}_{(j+1)N})\dot{\psi}_N$ from the superposition (20) are to be accounted at the equation for $\tilde{\boldsymbol{W}}$. Note that our convention in writing (36) is to drop the boundary terms with $\boldsymbol{e}_{0N}$ and $\boldsymbol{e}_{(M+1)N}$.

Substituting (36) to (29), all equations are satisfied up to the Nth order. At the N-th order, we divide (29) by ϵ^N and collect equations at the excited sites $n = jN$ for $j \in \{1, 2, ..., M\}$,

$$\begin{aligned}\ddot{\tilde{W}}_{jN} + V''(\varphi)\tilde{W}_{jN} &= (c_{j+1} + c_{j-1})\dot{\varphi}_{N-1} - \sigma_j(\sigma_{j+1} + \sigma_{j-1})c_j V'''(\varphi)\psi_N\dot{\varphi} \\ &\quad + \tilde{\lambda}^2 c_j(2\dot{v} - \dot{\varphi}) + \mathcal{O}(\epsilon^{1/2}),\end{aligned} \quad (37)$$

where we admit another convention that $\sigma_0 = \sigma_{M+1} = 0$ and $c_0 = c_{M+1} = 0$. In the derivation of equations (37), we have used the fact that the term $\dot{\varphi}_{N-1}$ comes from the fluxes from $n = (j+1)N$ and $n = (j-1)N$ sites generated by the derivatives of the linear inhomogeneous equations (18) and the term $\sigma_j(\sigma_{j+1} + \sigma_{j-1})c_j V'''(\varphi)\psi_N\dot{\varphi}$ comes from the expansion (20) of the nonlinear potential $V''(u_{jN})$.

Expanding $\tilde{\lambda} = \Lambda + \mathcal{O}(\epsilon^{1/2})$ and projecting the system of linear inhomogeneous equations (37) to $\dot{\varphi} \in H^2_{\mathrm{per}}(0,T)$, the kernel of $L = \partial_t^2 + V''(\varphi) : H^2_{\mathrm{per}}(0,T) \to L^2_{\mathrm{per}}(0,T)$, we obtain the system of difference equations,

$$\begin{aligned}\Lambda^2 c_j \int_0^T \left(\dot{\varphi}^2 + 2v\ddot{\varphi}\right)\mathrm{d}t &= (c_{j+1} + c_{j-1})\int_0^T \dot{\varphi}\dot{\varphi}_{N-1}\,\mathrm{d}t - \sigma_j(\sigma_{j+1} + \sigma_{j-1})c_j \\ &\quad \times \int_0^T V'''(\varphi)\psi_N\dot{\varphi}^2\,\mathrm{d}t,\end{aligned}$$

where the integration by parts is used to simplify the left-hand side. Differentiating the linear inhomogeneous equation (19) and projecting it to $\dot{\varphi}$, we infer that

$$\int_0^T V'''(\varphi)\psi_N\dot{\varphi}^2\,\mathrm{d}t = \int_0^T \dot{\varphi}\dot{\varphi}_{N-1}\,\mathrm{d}t \equiv K_N.$$

The system of difference equations yields the matrix eigenvalue problem (35) if we can verify that

$$\int_0^T \left(\dot{\varphi}^2 + 2v\ddot{\varphi}\right)\,\mathrm{d}t = -\frac{T^2(E)}{T'(E)}.$$

To do so, we note that $v \equiv 2L_e^{-1}\ddot{\varphi}$ is even in $t \in \mathbb{R}$, so that it is given by the exact solution,

$$v(t) = t\dot{\varphi}(t) + C\partial_E\varphi(t),$$

where $C \in \mathbb{R}$. From the condition of T-periodicity for $v(t)$ and $\dot{v}(t)$, we obtain

$$v(0) = v(T) = Ca'(E), \qquad \dot{v}(0) = 0 = \dot{v}(T) = T\ddot{\varphi}(0) - CT'(E)\ddot{\varphi}(0),$$

hence $C = T(E)/T'(E)$ and

$$\begin{aligned}\int_0^T \left(\dot{\varphi}^2 + 2v\ddot{\varphi}\right)\,\mathrm{d}t &= 2C\int_0^T \ddot{\varphi}\partial_E\varphi\,\mathrm{d}t = -C\int_0^T \left(\dot{\varphi}\partial_E\dot{\varphi} + V'(\varphi)\partial_E\varphi\right)\,\mathrm{d}t \\ &= -C\int_0^T \frac{\partial}{\partial E}\left(\frac{1}{2}\dot{\varphi}^2 + V(\varphi)\right)\,\mathrm{d}t = -CT(E) = -\frac{T^2(E)}{T'(E)},\end{aligned}$$

where equation (8) has been used. Finally, the matrix eigenvalue problem (35) defines $2M$ small eigenvalues that bifurcate from $\lambda = 0$ for small $\epsilon > 0$. The proof of the lemma is complete. □

We shall now count eigenvalues of the matrix eigenvalue problem (35) to classify stable and unstable configurations of multi-site breathers near the anti-continuum limit.

Lemma 3. *Let n_0 be the numbers of negative elements in the sequence $\{\sigma_j\sigma_{j+1}\}_{j=1}^{M-1}$. If $T'(E)K_N > 0$, the matrix eigenvalue problem (35) has exactly n_0 pairs of purely imaginary eigenvalues Λ and $M-1-n_0$ pairs of purely real eigenvalues μ counting their multiplicities, in addition to the double zero eigenvalue. If $T'(E)K_N < 0$, the conclusion changes to the opposite.*

Proof. We shall prove that the matrix $\mathcal{S}$ has exactly n_0 positive and $M-1-n_0$ negative eigenvalues counting their multiplicities, in addition to the simple zero eigenvalue. If this is the case, the assertion of the lemma follows from the correspondence $\Lambda^2 = -\frac{T'(E)K_N}{T^2(E)}\gamma$, where γ is an eigenvalue of $\mathcal{S}$.

Setting $c_j = \sigma_j b_j$, we rewrite the eigenvalue problem $\mathcal{S}\boldsymbol{c} = \gamma\boldsymbol{c}$ as the difference equation,

$$\sigma_j\sigma_{j+1}(b_{j+1} - b_j) + \sigma_j\sigma_{j-1}(b_{j-1} - b_j) = \gamma b_j, \qquad j \in \{1, 2, ..., M\}, \quad (38)$$

subject to the conditions $\sigma_0 = \sigma_{M+1} = 0$. Therefore, $\gamma = 0$ is always an eigenvalue with the eigenvector $\boldsymbol{b} = [1, 1, ..., 1] \in \mathbb{R}^M$. The coefficient matrix in (38) coincides with the one analysed by Sandstede in lemma 5.4 and appendix C [19]. This correspondence yields the assertion on the number of eigenvalues of $\mathcal{S}$. □

Before generalizing the results of lemmas 2 and 3 to other multi-site breathers, we consider two examples, which are related to the truncated potential (13). We shall use the Fourier cosine series for the solution $\varphi \in H^2_e(0, T)$,

$$\varphi(t) = \sum_{n\in\mathbb{N}} c_n(T)\cos\left(\frac{2\pi nt}{T}\right), \quad (39)$$

Table 1. Stable multi-site breathers in hard and soft potentials. The stability threshold T_N is found from the zero of K_N for $T \in (2\pi, 6\pi)$.

	N odd	N even
Hard potential $V'(u) = u + u^3$, $0 < T < 2\pi$	In-phase	Anti-phase
Soft potential $V'(u) = u - u^3$, $2\pi < T < 6\pi$	Anti-phase	$2\pi < T < T_N$ Anti-phase $T_N < T < 6\pi$ In-phase

for some square summable set $\{c_n(T)\}_{n\in\mathbb{N}}$. Because of the symmetry of V, we have $\varphi(T/4) = 0$, which imply that $c_n(T) \equiv 0$ for all even $n \in \mathbb{N}$. Solving the linear inhomogeneous equations (18), we obtain

$$\varphi_k(t) = \sum_{n\in\mathbb{N}_{\rm odd}} \frac{T^{2k} c_n(T)}{\left(T^2 - 4\pi^2 n^2\right)^k} \cos\left(\frac{2\pi n t}{T}\right), \qquad k \in \mathbb{N}. \tag{40}$$

Using Parseval's equality, we compute the constant K_N in lemma 2,

$$K_N = \int_0^T \dot{\varphi}(t)\dot{\varphi}_{N-1}(t)\,\mathrm{d}t = 4\pi^2 \sum_{n\in\mathbb{N}_{\rm odd}} \frac{T^{2N-3} n^2 |c_n(T)|^2}{\left(T^2 - 4\pi^2 n^2\right)^{N-1}}. \tag{41}$$

For the hard potential with $V'(u) = u + u^3$, we know from figure 1 that the period $T(E)$ is a decreasing function of E from $T(0) = 2\pi$ to $\lim_{E\to\infty} T(E) = 0$. Since $T'(E) < 0$ and $T(E) < 2\pi$, we conclude that $T'(E)K_N < 0$ if N is odd and $T'(E)K_N > 0$ if N is even. By lemma 3, if N is odd, the only stable configuration of the multi-site breathers is the one with all equal $\{\sigma_j\}_{j=1}^M$ (in-phase breathers), whereas if N is even, the only stable configuration of the multi-site breathers is the one with all alternating $\{\sigma_j\}_{j=1}^M$ (anti-phase breathers). This conclusion is shown in the first line of table 1.

For the soft potential with $V'(u) = u - u^3$, we know from figure 1 that the period $T(E)$ is an increasing function of E from $T(0) = 2\pi$ to $\lim_{E\to E_0} T(E) = \infty$, where $E_0 = \frac{1}{4}$. If $T(E)$ is close to 2π, then the first positive term in the series (41) dominates and $K_N > 0$ for all $N \in \mathbb{N}$. At the same time, $T'(E) > 0$ and lemma 3 implies that the only stable configuration of the multi-site breathers is the one with all alternating $\{\sigma_j\}_{j=1}^M$ (anti-phase breathers). The conclusion holds for any $T > 2\pi$ if N is odd, because $K_N > 0$ in this case.

This precise conclusion is obtained in theorem 3.6 of [17] in the framework of the DNLS equation (4). It is also in agreement with perturbative arguments in [2, 12], which are valid for $N = 1$ (all excited sites are adjacent on the lattice). To elaborate this point further, we show in the appendix the equivalence between the matrix eigenvalue problem (35) with $N = 1$ and the criteria used in [2, 12].

For even $N \in \mathbb{N}$, we observe a new phenomenon, which arise for the soft potentials with larger values of $T(E) > 2\pi$. To be specific, we restrict our consideration of multi-site breathers with the period T in the interval $(2\pi, 6\pi)$. Similar results can be obtained in the intervals $(6\pi, 10\pi)$, $(10\pi, 14\pi)$, and so on. For even $N \in \mathbb{N}$, there exists a period $T_N \in (2\pi, 6\pi)$ such that the constant K_N in (41) changes sign from $K_N > 0$ for $T \in (2\pi, T_N)$ to $K_N < 0$ for $T \in (T_N, 6\pi)$. When it happens, the conclusion on stability of the multi-site breather change directly to the opposite: the only stable configuration of the multi-site breathers is the one with all equal $\{\sigma_j\}_{j=1}^M$ (in-phase breathers). This conclusion is shown in the second line of table 1.

We conclude this section with the stability theorem for general multi-site breathers. For the sake of clarity, we formulate the theorem in the case when $T'(E) > 0$ and all $K_N > 0$,

which arises for the soft potential with odd N. Using lemma 3, the count can be adjusted to the cases of $T'(E) < 0$ and/or $K_N < 0$.

Theorem 2. *Let $\{n_j\}_{j=1}^M \subset \mathbb{Z}$ be an increasing sequence with $M \in \mathbb{N}$. Let $\boldsymbol{u}^{(\epsilon)} \in l^2(\mathbb{Z}, H_e^2(0,T))$ be a solution of the discrete Klein–Gordon equation (1) in theorem 1 with $\boldsymbol{u}^{(0)}(t) = \sum_{j=1}^M \sigma_j \varphi(t) \boldsymbol{e}_{n_j}$ for small $\epsilon > 0$. Let $\{\varphi_m\}_{m=0}^\infty$ be defined by the linear equations (18) starting with $\varphi_0 = \varphi$.*

Define $\{N_j\}_{j=1}^{M-1}$ and $\{K_{N_j}\}_{j=1}^{M-1}$ by $N_j = n_{j+1} - n_j$ and $K_{N_j} = \int_0^T \dot{\varphi}\dot{\varphi}_{N_j-1}\,\mathrm{d}t$. Assume $T'(E) > 0$ and $K_{N_j} > 0$ for all N_j.

Let n_0 be the numbers of negative elements in the sequence $\{\sigma_j\sigma_{j+1}\}_{j=1}^{M-1}$. The eigenvalue problem (29) at the discrete breather $\boldsymbol{u}^{(\epsilon)}$ has exactly n_0 pairs of purely imaginary eigenvalues λ and $M - 1 - n_0$ pairs of purely real eigenvalues λ counting their multiplicities, in addition to the double zero eigenvalue.

Proof. The limiting configuration $\boldsymbol{u}^{(0)}(t) = \sum_{j=1}^M \sigma_j \varphi(t) \boldsymbol{e}_{n_j}$ defines clusters of excited sites with equal distances N_j between the adjacent excited sites.

According to lemma 2, splitting of M double Jordan blocks associated to the decompositions (31) and (32) occurs into different orders of the perturbation theory, which are determined by the set $\{N_j\}_{j=1}^{M-1}$. At each order of the perturbation theory, the splitting of eigenvalues associated with one cluster with equal distance between the adjacent excited sites obeys the matrix eigenvalue problem (35), which leaves exactly one double eigenvalue at zero and yields symmetric pairs of purely real or purely imaginary eigenvalues, in accordance to the count of lemma 3.

The double zero eigenvalue corresponds to the eigenvector $\boldsymbol{W}$ and the generalized eigenvector $\boldsymbol{Z}$ generated by the translational symmetry of the multi-site breather bifurcating from a particular cluster of excited sites in the limiting configuration $\boldsymbol{u}^{(0)}$. The splitting of the double zero eigenvalue associated with a particular cluster happens at the higher orders in ϵ, when the fluxes from adjacent clusters reach each others. Since the end-point fluxes from the multi-site breathers are equivalent to the fluxes (22) generated from the fundamental breathers, they still obey lemma 1 and the splitting of double zero eigenvalue associated with different clusters still obeys lemma 2.

At the same time, the small pairs of real and imaginary eigenvalues arising at a particular order in ϵ remain at the real and imaginary axes in higher orders of the perturbation theory because their geometric and algebraic multiplicity coincides, thanks to the fact that these eigenvalues are related to the eigenvalues of the symmetric matrix $\mathcal{S}$ in the matrix eigenvalue problem (35).

Avoiding lengthy algebraic proofs, these arguments yield the assertion of the theorem. □

4. Numerical results

We illustrate our analytical results on existence and stability of discrete breathers near the anti-continuum limit by using numerical approximations. The discrete Klein–Gordon equation (1) can be truncated at a finite system of differential equations by applying the Dirichlet conditions at the ends.

4.1. Three-site model

The simplest model which allows gaps in the initial configuration $\mathbf{u}^{(0)}$ is the one restricted to three lattice sites, e.g. $n \in \{-1, 0, 1\}$. We choose the soft potential $V'(u) = u - u^3$ and rewrite the truncated discrete Klein–Gordon equation as a system of three Duffing oscillators

with linear coupling terms,

$$\begin{cases} \ddot{u}_0 + u_0 - u_0^3 = \epsilon(u_1 - 2u_0 + u_{-1}), \\ \ddot{u}_{\pm 1} + u_{\pm 1} - u_{\pm 1}^3 = \epsilon(u_0 - 2u_{\pm 1}). \end{cases} \tag{42}$$

A fast and accurate approach to construct T-periodic solutions for this system is the shooting method. The idea is to find $\mathbf{a} \in \mathbb{R}^3$ such that the solution $\mathbf{u}(t) \in C^1(\mathbb{R}_+, \mathbb{R}^3)$ with initial conditions $\mathbf{u}(0) = \mathbf{a}$, $\dot{\mathbf{u}}(0) = 0$ satisfy the conditions of T-periodicity, $\mathbf{u}(T) = \mathbf{a}$, $\dot{\mathbf{u}}(T) = 0$. However, these constraints would generate an over-determined system of equations on $\mathbf{a}$. To set up the square system of equations, we can use the symmetry $t \mapsto -t$ of system (42). If we add the constraint $\dot{\mathbf{u}}(T/2) = 0$, then even solutions of system (42) satisfy $\mathbf{u}(-T/2) = \mathbf{u}(T/2)$ and $\dot{\mathbf{u}}(-T/2) = -\dot{\mathbf{u}}(T/2) = 0$, that is, these solutions are T-periodic. Hence, the values of $\mathbf{a} \in \mathbb{R}^3$ become the roots of the vector $\boldsymbol{F}(\mathbf{a}) = \dot{\mathbf{u}}(T/2) \in \mathbb{R}^3$.

We now construct a periodic solution $\mathbf{u}$ to system (42) that corresponds to the anti-continuum limit $\mathbf{u}^{(0)}$ as follows. Using the initial data $\mathbf{u}^{(0)}(0)$ as an initial guess for the shooting method for a fixed value of T, we continue the initial displacement $\mathbf{u}(0)$ with respect to the coupling constant $\epsilon > 0$. After that, we fix a value of ϵ and use the shooting method again to continue the initial displacement $\mathbf{u}(0)$ with respect to period T.

Let us apply this method to determine initial conditions for the fundamental breather,

$$u_0^{(0)} = \varphi, \qquad u_{\pm 1}^{(0)} = 0, \tag{43}$$

and for a two-site breather with a hole,

$$u_0^{(0)} = 0, \qquad u_{\pm 1}^{(0)} = \varphi. \tag{44}$$

In both cases, we can use the symmetry $u_{-1}(t) = u_1(t)$ to reduce the dimension of the shooting method to two unknowns a_0 and a_1.

Figure 2 shows solution branches for these two breathers on the period–amplitude plane by plotting T versus a_0 and a_1 for $\epsilon = 0.01$. For $2\pi < T < 6\pi$, solution branches are close to the limiting solutions (dotted line), in agreement with theorem 1. However, a new phenomenon emerges near $T = 6\pi$: both breather solutions experience a pitchfork bifurcation and two more solution branches split off the main solution branch. The details of the pitchfork bifurcation for the fundamental solution branch are shown on the insets of figure 2.

Let T_S be the period at the point of the pitchfork bifurcation. We may think intuitively that T_S should approach to the point of $1:3$ resonance for small ϵ, that is, $T_S \to 6\pi$ as $\epsilon \to 0$. We have checked numerically that this conjecture is in fact false and the value of T_S gets larger as ϵ gets smaller. This property of the pitchfork bifurcation is analysed in section 5 (see remark 5 and figure 12).

Figure 2 also shows two branches of solutions for $T > 6\pi$ with negative values of a_1 for positive values of a_0 and vice versa. One of the two branches is close to the breathers at the anti-continuum limit, as prescribed by theorem 1. We note that the breather solutions prescribed by theorem 1 for $T < 6\pi$ and $T > 6\pi$ belong to different solution branches. This property is also analysed in section 5 (see remark 4 and figure 9).

Figure 3 shows the fundamental breather before ($T = 5\pi$) and after ($T = 5.8\pi$) pitchfork bifurcation. The symmetry condition $\mathbf{u}(T/4) = 0$ for the solution at the main branch is violated for two new solutions that bifurcate from the main branch. Note that the two new solutions bifurcating for $T > T_S$ look different on the graphs of a_0 and a_1 versus T. Nevertheless, these two solutions are related to each other by the symmetry of the system (42). If $\mathbf{u}(t)$ is one solution of the system (42), then $-\mathbf{u}(t + T/2)$ is another solution of the same system. If $\mathbf{u}(T/4) \neq 0$, then these two solutions are different from each other.

Let us now illustrate the stability result of theorem 2 using the fundamental breather (43) and the breather with a hole (44). We draw a conclusion on linearized stability of the breathers

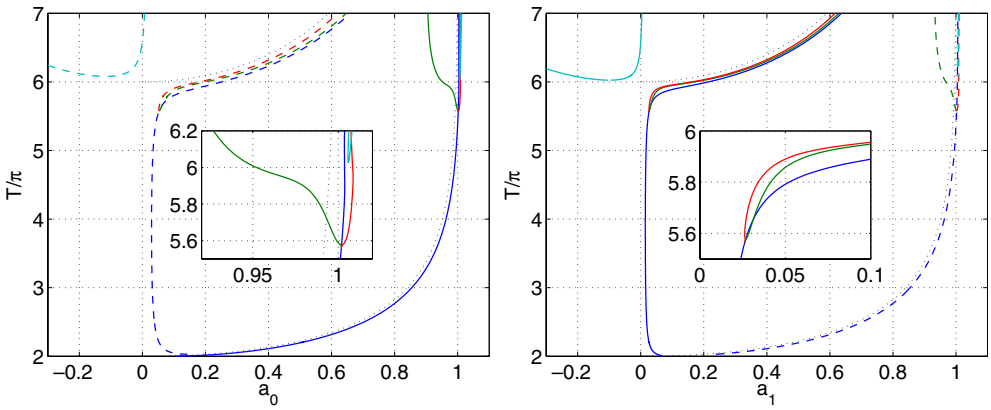

Figure 2. The initial displacements a_0 and a_1 for the T-periodic solutions to system (42) with $\epsilon = 0.01$. The solid and dashed lines correspond to the fundamental (43) and two-site (44) breathers respectively. The dotted lines correspond to the T-periodic solutions to equation (8). The insets show the pitchfork bifurcation of the fundamental breather.

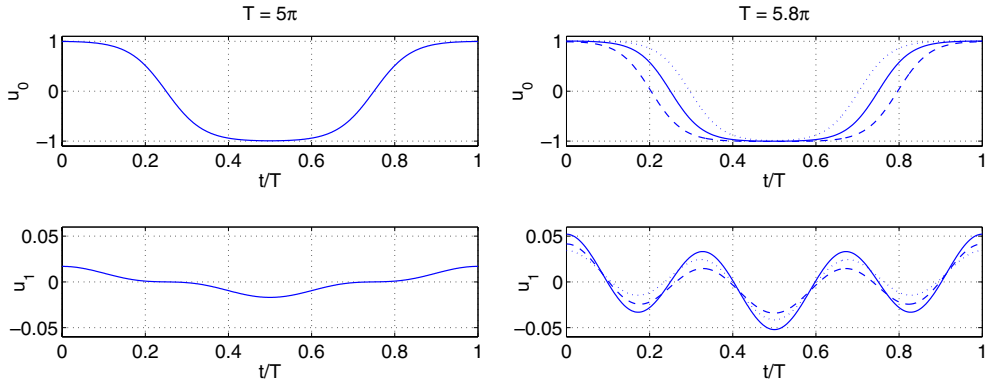

Figure 3. Fundamental breathers for system (42) before (left) and after (right) the symmetry-breaking bifurcation at $\epsilon = 0.01$.

by testing whether their Floquet multipliers, found from the monodromy matrix associated with the linearization of system (42), stay on the unit circle.

Figure 4 shows the real part of Floquet multipliers versus the breather's period for the fundamental breather (left) and the new solution branches (right) bifurcating from the fundamental breather due to the pitchfork bifurcation. Because Floquet multipliers are on the unit circle for all periods below the bifurcation value T_S, the fundamental breather remains stable for these periods, in agreement with theorem 2. Once the bifurcation occurs, one of the Floquet multiplier becomes real and unstable (outside the unit circle). Two new stable solutions appear during the bifurcation and have the identical Floquet multipliers because of the aforementioned symmetry between the new solutions. These solutions become unstable for periods slightly larger than the bifurcation value T_S, because of the period-doubling bifurcation associated with Floquet multipliers at -1.

We perform similar computations for the two-site breather with the central hole (44). Figure 5 (left) shows that at the coupling $\epsilon = 0.01$ the breather is unstable for periods $2\pi < T < T_*^{(\epsilon)}$ and stable for periods $T \gtrapprox T_*^{(\epsilon)}$ with $T_*^{(\epsilon)} \approx 5.425\pi$ for $\epsilon = 0.01$. This can be compared using the change of stability predicted by theorem 2. According to equation (41),

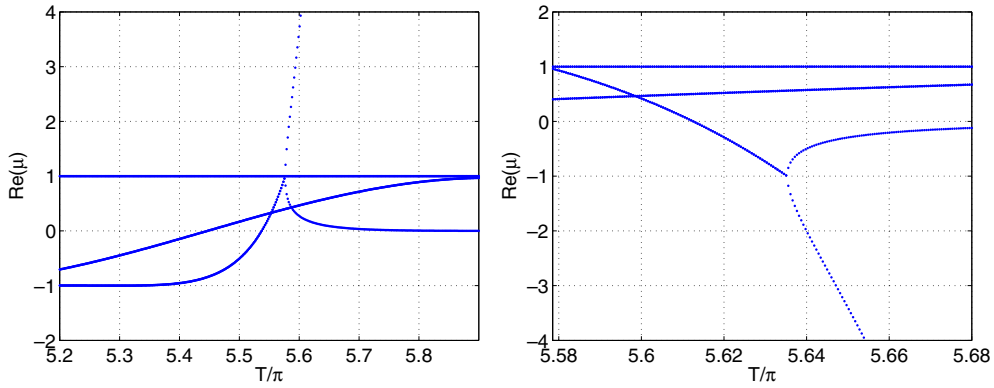

Figure 4. Real parts of Floquet multipliers μ for the fundamental breather at $\epsilon = 0.01$ near the bifurcation for the main branch (left) and side branches (right).

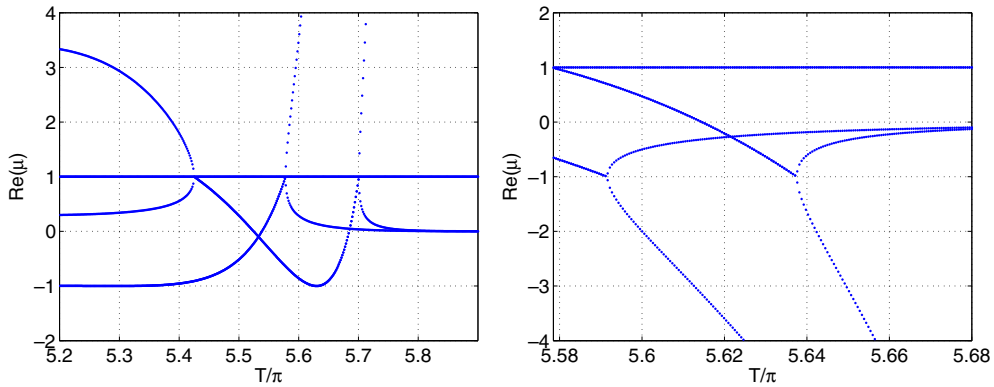

Figure 5. Real parts of Floquet multipliers μ for the two-site breather with a hole at $\epsilon = 0.01$ near the bifurcation for the main branch (left) and side branches (right).

K_2 changes sign from positive to negative at $T_{N=2} \approx 5.476\pi$. Since $T'(E)$ is positive for the soft potential, theorem 2 predicts that in the anti-continuum limit the two-site breather is unstable for $2\pi < T < T_{N=2}$ and stable for $T_{N=2} < T < 6\pi$. This change of stability agrees with figure 5 where we note that $|T_*^{(\epsilon)} - T_{N=2}| \approx 0.05\pi$ at $\epsilon = 0.01$.

At $T \approx 5.6\pi$ and $T \approx 5.7\pi$, two bifurcations occur for the two-site breather with the central hole and unstable multipliers bifurcate from the unit multiplier for larger values of T. The behaviour of Floquet multipliers is similar to the one in figure 4 (left) and it marks two consequent pitchfork bifurcations for the two-site breather with the hole. The first bifurcation is visible in figure 2 in the space of symmetric two-site breathers with $u_{-1}(t) = u_1(t)$. The Floquet multipliers for the side branches of these symmetric two-site breathers is shown in figure 5 (right), where we can see two consequent period-doubling bifurcations in comparison with one such bifurcation in figure 4 (right). The second bifurcation is observed in the space of asymmetric two-site breathers with $u_{-1}(t) \neq u_1(t)$.

We display the two pitchfork bifurcations on the top panel of figure 6. One can see for the second bifurcation that the value of a_0 is the same for both breathers splitting of the main solution branch. Although the values of a_{-1} and a_1 look same for the second bifurcation, dashed and dotted lines indicate that a_1 is greater than a_{-1} at one asymmetric branch and vice

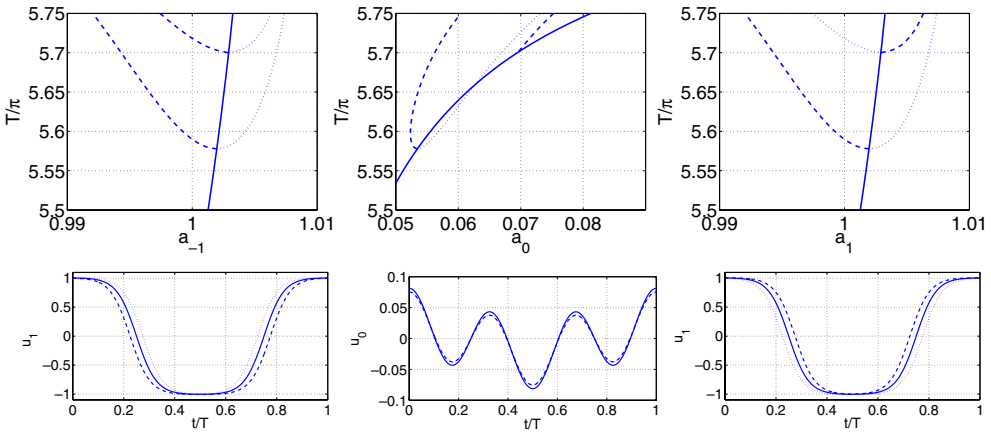

Figure 6. Top: the initial displacements a_{-1}, a_0, and a_1 for the T-periodic breather with a hole on the three-site lattice with $\epsilon = 0.01$. Bottom: asymmetric breathers with period $T = 5.75\pi$ on the three-site lattice with $\epsilon = 0.01$.

versa for the other one. The bottom panels of figure 6 show the asymmetric breathers with period $T = 5.75\pi$ that appear as a result of the second pitchfork bifurcation.

4.2. Five-site model

We can now truncate the discrete Klein–Gordon equation (1) at five lattice sites, e.g. at $n \in \{-2, -1, 0, 1, 2\}$. The fundamental breather (43) and the breather with a central hole (44) are continued in the five-site lattice subject to the symmetry conditions $u_n(t) = u_{-n}(t)$ for $n = 1, 2$. We would like to illustrate that increasing the size of the lattice does not qualitatively change the previous existence and stability results, in particular, the properties of the pitchfork bifurcations.

Figure 7 gives analogues of figure 2 for the fundamental breather and the breather with a hole. The associated Floquet multipliers are shown in figure 8, in full analogy with figures 4 and 5. We can see that both existence and stability results are analogous between the three-site and five-site lattices.

5. Pitchfork bifurcation near 1 : 3 resonance

We study here the symmetry-breaking (pitchfork) bifurcation of the fundamental breather. This bifurcation illustrated in figure 3 occurs for soft potentials near the point of 1 : 3 resonance, when the period T is close to 6π. We point out that the period T_S of the pitchfork bifurcation is close to 6π for small but finite values of ϵ. As we have discovered numerically, T_S gets larger as ϵ gets smaller. This property indicates that the asymptotic analysis of this bifurcation is not uniform with respect to two small parameters ϵ and $T - 6\pi$, which we explain below in more details.

When $\boldsymbol{u} = \phi^{(\epsilon)}$ is the fundamental breather and $T \neq 2\pi n$ is fixed, theorem 1 and lemma 1 imply that

$$\begin{cases} u_0(t) &= \varphi(t) - 2\epsilon\psi_1(t) + \mathcal{O}_{H^2_{\rm per}(0,T)}(\epsilon^2), \\ u_{\pm1}(t) &= \epsilon\varphi_1(t) + \mathcal{O}_{H^2_{\rm per}(0,T)}(\epsilon^2), \\ u_{\pm n}(t) &= \mathcal{O}_{H^2_{\rm per}(0,T)}(\epsilon^2), \qquad n \geqslant 2, \end{cases} \tag{45}$$

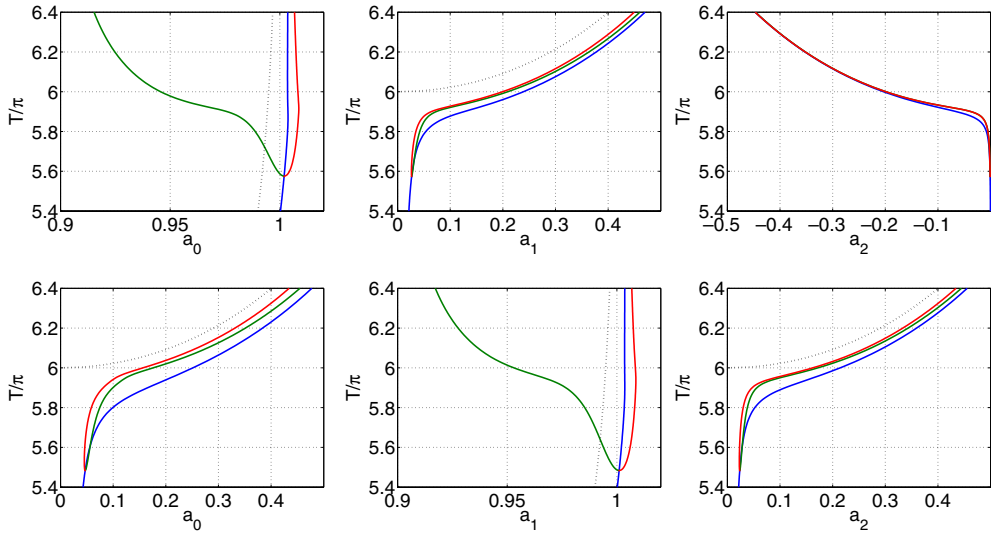

Figure 7. Top: the initial displacements a_0, a_1, and a_2 for the T-periodic fundamental breather of the five-site lattice with $\epsilon = 0.01$. Bottom: the same for the two-site breather with a hole. The dotted lines correspond to the T-periodic solutions to equation (8).

where φ can be expanded in the Fourier series,

$$\varphi(t) = \sum_{n \in \mathbb{N}_{\text{odd}}} c_n(T) \cos\left(\frac{2\pi n t}{T}\right), \tag{46}$$

and the Fourier coefficients $\{c_n(T)\}_{n \in \mathbb{N}_{\text{odd}}}$ are uniquely determined by the period T. The correction terms φ_1 and ψ_1 are determined by the solution of the linear inhomogeneous equations (18) and (19), in particular, we have

$$\varphi_1(t) = \sum_{n \in \mathbb{N}_{\text{odd}}} \frac{T^2 c_n(T)}{T^2 - 4\pi^2 n^2} \cos\left(\frac{2\pi n t}{T}\right). \tag{47}$$

In what follows, we restrict our consideration of soft potentials to the case of the quartic potential $V'(u) = u - u^3$. We shall assume that $c_3(6\pi) \neq 0$ and the numerical approximations suggest that $c_3(6\pi) < 0$ for the quartic potential.

Expansion (45) and solution (47) imply that if T is fixed in $(2\pi, 6\pi)$, then $\|u_{\pm 1}\|_{H^2_{\text{per}}(0,T)} = \mathcal{O}(\epsilon)$ and the cubic term $u^3_{\pm 1}$ is neglected at the order $\mathcal{O}(\epsilon)$, where the linear inhomogeneous equation (18) is valid. Near the resonant period $T = 6\pi$, the norm $\|u_{\pm 1}\|_{H^2_{\text{per}}(0,T)}$ is much larger than $\mathcal{O}(\epsilon)$ if $c_3(6\pi) \neq 0$. As a result, the cubic term $u^3_{\pm 1}$ must be incorporated at the leading order of the asymptotic approximation.

We shall reduce the discrete Klein–Gordon equation (1) for the fundamental breather near 1 : 3 resonance to a normal form equation, which coincides with the nonlinear Duffing oscillator perturbed by a small harmonic forcing (equation (66)). The normal form equation features the same properties of the pitchfork bifurcation of T-periodic solutions as the discrete Klein–Gordon equation (1). To prepare for the reduction to the normal form equation, we introduce the scaling transformation,

$$T = \frac{6\pi}{1 + \delta\epsilon^{2/3}}, \quad \tau = (1 + \delta\epsilon^{2/3})t, \quad u_n(t) = (1 + \delta\epsilon^{2/3})U_n(\tau), \tag{48}$$

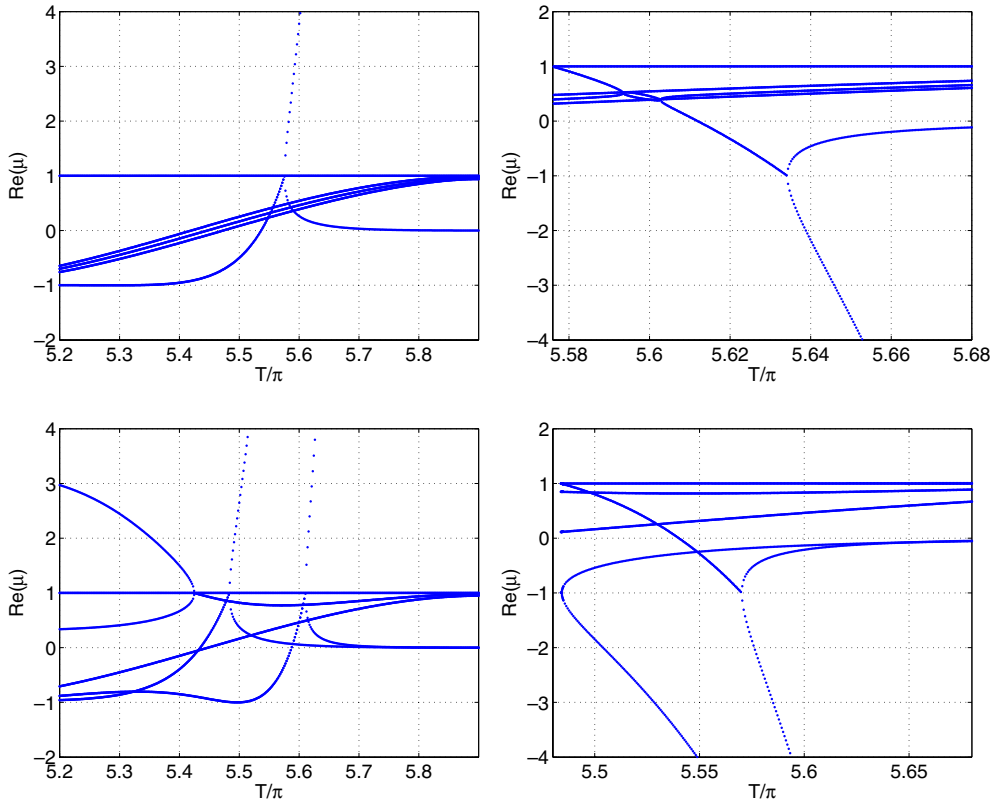

Figure 8. Top: real parts of Floquet multipliers μ for the fundamental breather near the bifurcation for the main branch (left) and side branches (right). Bottom: the same for the two-site breather with a hole.

where δ is a new parameter, which is assumed to be ϵ-independent. The discrete Klein–Gordon equation (1) with $V'(u) = u - u^3$ can be rewritten in new variables (48) as follows,

$$\ddot{U}_n + U_n - U_n^3 = \beta U_n + \gamma(U_{n+1} + U_{n-1}), \qquad n \in \mathbb{Z}, \tag{49}$$

where

$$\beta = 1 - \frac{1 + 2\epsilon}{(1 + \delta\epsilon^{2/3})^2}, \qquad \gamma = \frac{\epsilon}{(1 + \delta\epsilon^{2/3})^2}. \tag{50}$$

T-periodic solutions of the discrete Klein–Gordon equation (1) in variables $\{u_n(t)\}_{n\in\mathbb{Z}}$ become now 6π-periodic solutions of the rescaled Klein–Gordon equation (49) in variables $\{U_n(\tau)\}_{n\in\mathbb{Z}}$. To reduce the system of Klein–Gordon equation (49) to the Duffing oscillator perturbed by a small harmonic forcing near $1:3$ resonance, we consider the fundamental breather, for which $U_n = U_{-n}$ for all $n \in \mathbb{N}$. Using this reduction, we write equations (49) separately at $n = 0$, $n = 1$ and $n \geqslant 2$:

$$\ddot{U}_0 + U_0 - U_0^3 = \beta U_0 + 2\gamma U_1, \tag{51}$$

$$\ddot{U}_1 + U_1 - U_1^3 = \beta U_1 + \gamma U_2 + \gamma U_0, \tag{52}$$

$$\ddot{U}_n + U_n - U_n^3 = \beta U_n + \gamma(U_{n+1} + U_{n-1}), \qquad n \geqslant 2. \tag{53}$$

Let us represent a 6π-periodic function U_0 with the symmetries

$$U_0(-\tau) = U_0(\tau) = -U_0(3\pi - \tau), \qquad \tau \in \mathbb{R}, \tag{54}$$

by the Fourier series,

$$U_0(\tau) = \sum_{n\in\mathbb{N}_{\rm odd}} b_n \cos\left(\frac{n\tau}{3}\right), \tag{55}$$

where $\{b_n\}_{n\in\mathbb{N}_{\rm odd}}$ are some Fourier coefficients. If U_0 converges to φ in H^2-norm as $\epsilon \to 0$ (when $\beta, \gamma \to 0$), then $b_n \to c_n(6\pi)$ as $\epsilon \to 0$ for all $n \in \mathbb{N}_{\rm odd}$, where the Fourier coefficients $\{c_n(6\pi)\}_{n\in\mathbb{N}_{\rm odd}}$ are uniquely defined by the Fourier series (46) for $T = 6\pi$. We assume again that $c_3(6\pi) \neq 0$ and δ is fixed independently of small $\epsilon > 0$.

We shall now use a Lyapunov–Schmidt reduction method to show that the components $\{U_n\}_{n\in\mathbb{N}}$ are uniquely determined from the system (52) and (53) for small $\epsilon > 0$ if U_0 is represented by the Fourier series (55). To do so, we decompose the solution into two parts:

$$U_n(\tau) = A_n \cos(\tau) + V_n(\tau), \qquad n \in \mathbb{N}, \tag{56}$$

where $V_n(\tau)$ is orthogonal to $\cos(\tau)$ in the sense $\langle V_n, \cos(\cdot)\rangle_{L^2_{\rm per}(0,6\pi)} = 0$. Projecting the system (52) and (53) to $\cos(\tau)$, we obtain a difference equation for $\{A_n\}_{n\in\mathbb{N}}$:

$$\beta A_1 + \gamma A_2 + \gamma b_3 = -\frac{1}{3\pi}\int_0^{6\pi} \cos(\tau)(A_1\cos(\tau) + V_1(\tau))^3\,{\rm d}\tau, \tag{57}$$

$$\beta A_n + \gamma(A_{n+1} + A_{n-1}) = -\frac{1}{3\pi}\int_0^{6\pi} \cos(\tau)(A_n\cos(\tau) + V_n(\tau))^3\,{\rm d}\tau, \qquad n \geqslant 2. \tag{58}$$

Projecting the system (52) and (53) to the orthogonal complement of $\cos(\tau)$, we obtain a lattice differential equation for $\{V_n(\tau)\}_{n\in\mathbb{N}}$:

$$\begin{aligned}\ddot{V}_1 + V_1 &= \beta V_1 + \gamma V_2 + \gamma \sum_{k\in\mathbb{N}_{\rm odd}\setminus\{3\}} b_k \cos\left(\frac{k\tau}{3}\right) \\ &\quad + (A_1\cos(\tau) + V_1)^3 - \cos(\tau)\frac{\langle\cos(\cdot), (A_1\cos(\cdot) + V_1)^3\rangle_{L^2_{\rm per}(0,6\pi)}}{\langle\cos(\cdot),\cos(\cdot)\rangle_{L^2_{\rm per}(0,6\pi)}},\end{aligned} \tag{59}$$

$$\begin{aligned}\ddot{V}_n + V_n &= \beta V_n + \gamma(V_{n+1} + V_{n-1}) \\ &\quad + (A_n\cos(\tau) + V_n)^3 - \cos(\tau)\frac{\langle\cos(\cdot), (A_n\cos(\cdot) + V_n)^3\rangle_{L^2_{\rm per}(0,6\pi)}}{\langle\cos(\cdot),\cos(\cdot)\rangle_{L^2_{\rm per}(0,6\pi)}}, \qquad n \geqslant 2.\end{aligned} \tag{60}$$

Recall that $\beta = \mathcal{O}(\epsilon^{2/3})$ and $\gamma = \mathcal{O}(\epsilon)$ as $\epsilon \to 0$ if δ is fixed independently of small $\epsilon > 0$. Provided that the sequence $\{A_n\}_{n\in\mathbb{N}}$ is bounded and $\|\boldsymbol{A}\|_{l^\infty(\mathbb{N})}$ is small as $\epsilon \to 0$, the implicit function theorem applied to the system (59) and (60) yields a unique even solution for $\boldsymbol{V} \in l^2(\mathbb{N}, H^2_e(0, 6\pi))$ such that $\langle \boldsymbol{V}, \cos(\cdot)\rangle_{L^2_{\rm per}(0,6\pi)} = \boldsymbol{0}$ in the neighbourhood of zero solution for small $\epsilon > 0$ and $\boldsymbol{A} \in l^\infty(\mathbb{N})$. Moreover, for all small $\epsilon > 0$ and $\boldsymbol{A} \in l^\infty(\mathbb{N})$, there is a positive constant $C > 0$ such that

$$\|\boldsymbol{V}\|_{l^2(\mathbb{N}, H^2_{\rm per}(0,6\pi))} \leqslant C(\epsilon + \|\boldsymbol{A}\|^3_{l^\infty(\mathbb{N})}). \tag{61}$$

The balance occurs if $\|\boldsymbol{A}\|_{l^\infty(\mathbb{N})} = \mathcal{O}(\epsilon^{1/3})$ as $\epsilon \to 0$.

Recall now that $\beta = 2\delta\epsilon^{2/3} - 2\epsilon + \mathcal{O}(\epsilon^{4/3})$ and $\gamma = \epsilon + \mathcal{O}(\epsilon^{5/3})$ as $\epsilon \to 0$. Substituting the solution of the system (59) and (60) satisfying (61) to the system (57) and (58) and using the scaling transformation $A_n = \epsilon^{1/3} a_n$, $n \in \mathbb{N}$, we obtain the perturbed difference equation for $\{a_n\}_{n\in\mathbb{N}}$:

$$2\delta a_1 + \frac{3}{4}a_1^3 + b_3 = \epsilon^{1/3}(2a_1 - a_2) + \mathcal{O}(\epsilon^{2/3}), \tag{62}$$

$$2\delta a_n + \frac{3}{4}a_n^3 = \epsilon^{1/3}(2a_n - a_{n+1} - a_{n-1}) + \mathcal{O}(\epsilon^{2/3}), \qquad n \geqslant 2. \tag{63}$$

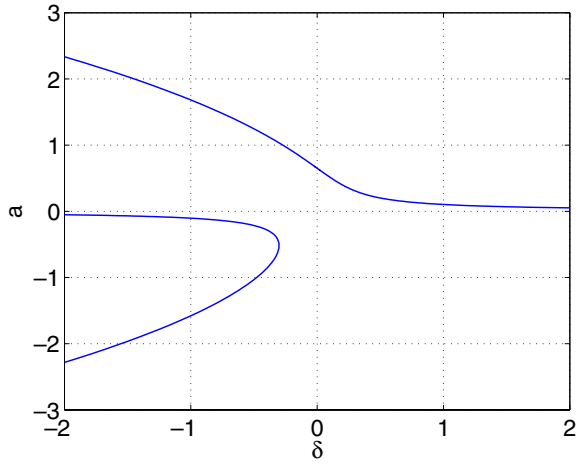

Figure 9. Roots of the cubic equation (64).

At $\epsilon = 0$, the system (62) and (63) is decoupled. Let $a(\delta)$ be a root of the cubic equation:

$$2\delta a(\delta) + \frac{3}{4}a^3(\delta) + c_3(6\pi) = 0, \tag{64}$$

where $c_3(6\pi) \neq 0$ is given. Roots of the cubic equation (64) are shown in figure 9 for $c_3(6\pi) < 0$. A positive root continues across $\delta = 0$ and the two negative roots bifurcate for $\delta < 0$ by means of a saddle-node bifurcation.

Let $a(\delta)$ denote any root of cubic equation (64) such that $8\delta + 9a^2(\delta) \neq 0$. Assuming that $b_3 = c_3(6\pi) + \mathcal{O}(\epsilon^{2/3})$ as $\epsilon \to 0$ (this assumption is proved later in lemma 5), the implicit function theorem yields a unique continuation of this root in the system (62) and (63) for small $\epsilon > 0$ and any fixed $\delta \neq 0$:

$$\begin{cases} a_1 = a(\delta) + \epsilon^{1/3}\frac{8a(\delta)}{8\delta+9a^2(\delta)} + \mathcal{O}(\epsilon^{2/3}), \\ a_2 = \quad -\epsilon^{1/3}\frac{a(\delta)}{2\delta} \quad + \mathcal{O}(\epsilon^{2/3}), \\ a_n = \qquad\qquad\quad + \mathcal{O}(\epsilon^{2/3}), \qquad n \geqslant 3. \end{cases} \tag{65}$$

Again, these expansions are valid for any fixed $\delta \neq 0$ such that $8\delta + 9a^2(\delta) \neq 0$.

Remark 3. The condition $8\delta + 9a^2(\delta) = 0$ implies bifurcations among the roots of the cubic equation (64), e.g. the fold bifurcation, when two roots coalesce and disappear after δ crosses a bifurcation value. The condition $\delta = 0$ does not lead to new bifurcations but implies that the value of a_2 is no longer as small as $\mathcal{O}(\epsilon^{1/3})$. Refined scaling shows that if $\delta = 0$, then $a_1 = a(0) + \mathcal{O}(\epsilon^{1/3})$, $a_2 = \mathcal{O}(\epsilon^{1/9})$, and $a_n = \mathcal{O}(\epsilon^{4/27})$, $n \geqslant 3$, where $a(0)$ is a unique real root of the cubic equation (64) for $\delta = 0$.

We can now focus on the last remaining equation (51) of the rescaled discrete Klein–Gordon equation (49). Substituting $U_1 = \epsilon^{1/3}a(\delta)\cos(\tau) + \mathcal{O}_{H^2_{\rm per}(0,6\pi)}(\epsilon^{2/3})$ into equation (51), we obtain the perturbed normal form for 1 : 3 resonance,

$$\ddot{U}_0 + U_0 - U_0^3 = \beta U_0 + \nu\cos(\tau) + \mathcal{O}_{H^2_{\rm per}(0,6\pi)}(\epsilon^{5/3}), \tag{66}$$

where $\nu = 2\gamma\epsilon^{1/3}a(\delta) = \mathcal{O}(\epsilon^{4/3})$ as $\epsilon \to 0$. Because $a(\delta) \neq 0$, we know that $\nu \neq 0$ if $\epsilon \neq 0$. The perturbed normal form (66) coincides with the nonlinear Duffing oscillator perturbed by a small harmonic forcing. The following lemma summarizes the reduction of the discrete

Klein–Gordon equation to the perturbed Duffing equation, which was proved above with the Lyapunov–Schmidt reduction arguments.

Lemma 4. *Let $\delta \neq 0$ be fixed independently of small $\epsilon > 0$. Let $a(\delta)$ be a root of the cubic equation (64) such that $8\delta + 9a^2(\delta) \neq 0$. Assume that $c_3(6\pi) \neq 0$ among the Fourier coefficients (46). For any 6π-periodic solution U_0 of the perturbed Duffing equation (66) satisfying symmetries (54) such that*

$$U_0(\tau) = \varphi(\tau) + \mathcal{O}_{H^2_{\rm per}(0,6\pi)}(\epsilon^{2/3}) \quad \text{as} \qquad \epsilon \to 0, \tag{67}$$

there exists a solution of the discrete Klein–Gordon equation (49) such that

$$\begin{cases} U_{\pm 1}(\tau) = \epsilon^{1/3} a(\delta)\cos(\tau) + \epsilon^{2/3}\frac{8a(\delta)}{8\delta+9a^2(\delta)}\cos(\tau) + \mathcal{O}_{H^2_{\rm per}(0,6\pi)}(\epsilon), \\ U_{\pm 2}(\tau) = \qquad\qquad - \epsilon^{2/3}\frac{a(\delta)}{2\delta}\cos(\tau) \qquad + \mathcal{O}_{H^2_{\rm per}(0,6\pi)}(\epsilon), \\ U_{\pm n}(\tau) = \qquad\qquad\qquad\qquad\quad + \mathcal{O}_{H^2_{\rm per}(0,6\pi)}(\epsilon), \qquad n \geqslant 3. \end{cases} \tag{68}$$

Remark 4. Figure 9 shows that two negative roots of the cubic equation (64) bifurcate at $\delta_* < 0$ via the saddle-node bifurcation and exist for $\delta < \delta_*$. Negative values of δ correspond to $T > 6\pi$. As ϵ is small, this saddle-node bifurcation gives a birth of two periodic solutions with

$$u_1(0) = \epsilon^{1/3} a(\delta) + \mathcal{O}(\epsilon^{2/3}) < 0.$$

This bifurcation is observed in figure 2 (right), one of the two new solutions still satisfies the asymptotic representation (45) as $\epsilon \to 0$ for fixed $T > 6\pi$.

In what follows, we shall consider the positive root of the cubic equation (64) that continues across $\delta = 0$. We are interested in 6π-periodic solutions of the perturbed normal form (66) in the limit of small $\epsilon > 0$ (when $\beta = \mathcal{O}(\epsilon^{2/3})$ and $\nu = \mathcal{O}(\epsilon^{4/3})$ are small). Since the remainder term is small as $\epsilon \to 0$ and the persistence analysis is rather straightforward, we obtain main results by studying the truncated Duffing equation with a small harmonic forcing:

$$\ddot{U} + U - U^3 = \beta U + \nu\cos(\tau). \tag{69}$$

The following lemma guarantees the persistence of 6π-periodic solutions with even symmetry in the Duffing equation (69) for small values of β and ν. Note that this persistence is assumed in equation (67) of the statement of lemma 4.

Lemma 5. *There are positive constants β_0, ν_0, and C such that for all $\beta \in (-\beta_0, \beta_0)$ and $\nu \in (-\nu_0, \nu_0)$, the normal form equation (69) admits a unique 6π-periodic solution $U_{\beta,\nu} \in H^2_e(0, 6\pi)$ satisfying symmetries*

$$U_{\beta,\nu}(-\tau) = U_{\beta,\nu}(\tau) = -U_{\beta,\nu}(3\pi - \tau), \qquad \tau \in \mathbb{R}, \tag{70}$$

and bound

$$\|U_{\beta,\nu} - \varphi\|_{H^2_{\rm per}} \leqslant C(|\beta| + |\nu|). \tag{71}$$

Moreover, the map $\mathbb{R} \times \mathbb{R} \ni (\beta, \nu) \mapsto U_{\beta,\nu} \in H^2_e(0, 6\pi)$ is C^∞ for all $\beta \in (-\beta_0, \beta_0)$ and $\nu \in (-\nu_0, \nu_0)$.

Proof. The proof follows by the Lyapunov–Schmidt reduction arguments. For $\nu = 0$ and small $\beta \in (-\beta_0, \beta_0)$, there exists a unique 6π-periodic solution $U_{\beta,0}$ satisfying the symmetry (70), which is $\mathcal{O}(\beta)$-close to φ in the $H^2_{\rm per}(0, 6\pi)$ norm. Because the Duffing oscillator is non-degenerate, the Jacobian operator $L_{\beta,0}$ has a one-dimensional kernel spanned by the odd function $\dot{U}_{\beta,0}$, where

$$L_{\beta,\nu} = \partial_t^2 + 1 - \beta - 3U^2_{\beta,\nu}(t). \tag{72}$$

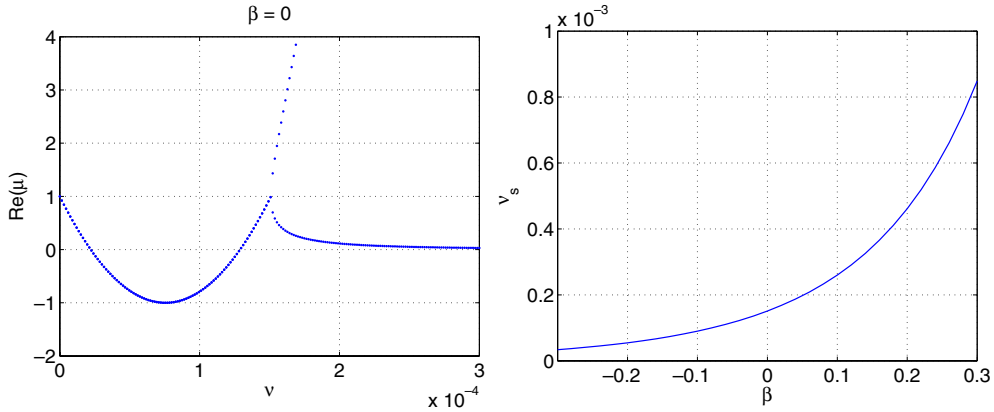

Figure 10. Left: Floquet multipliers μ of equation $L_{\beta,\nu}W = 0$. Right: parameter ν versus β at the symmetry-breaking bifurcation.

Therefore, $\langle \dot{U}_{\beta,0}, \cos(\cdot)\rangle_{L^2_{\rm per}(0,6\pi)} = 0$, and the unique even solution persists for small $\nu \in (-\nu_0, \nu_0)$. The symmetry (70) persists for all $\nu \in (-\nu_0, \nu_0)$ because both the Duffing oscillator and the forcing term $\cos(\tau)$ satisfy this symmetry. □

Remark 5. Lemma 5 excludes the pitchfork bifurcation in the limit $\epsilon \to 0$ for fixed $\delta \neq 0$. This result implies that the period of the pitchfork bifurcation T_S does not converge to 6π as $\epsilon \to 0$. Indeed, we mentioned in the context of figure 2 that T_S gets larger as ϵ gets smaller.

By the perturbation theory arguments, the kernel of the Jacobian operator $L_{\beta,\nu}$ is empty for small β and ν provided that $\nu \neq 0$. Indeed, expanding the solution of lemma 5 in power series in β and ν, we obtain

$$U_{\beta,\nu} = \varphi + \beta L_e^{-1}\varphi + \nu L_e^{-1}\cos(\cdot) + \mathcal{O}_{H^2_{\rm per}(0,6\pi)}(\beta^2, \nu^2), \tag{73}$$

where L_e is the operator in (19). Although L_e has a one-dimensional kernel spanned by $\dot{\varphi}$, this eigenfunction is odd in τ, whereas φ and $\cos(\cdot)$ are defined in the space of even functions. Expanding potentials of the operator $L_{\beta,\nu}$, we obtain

$$L_{\beta,\nu}\dot{U}_{\beta,\nu} = \nu\sin(\cdot) + \mathcal{O}_{H^2_{\rm per}(0,6\pi)}(\beta^2, \nu^2). \tag{74}$$

We note that

$$\langle \dot{\varphi}, \sin(\cdot)\rangle_{L^2_{\rm per}(0,6\pi)} = -\langle \varphi, \cos(\cdot)\rangle_{L^2_{\rm per}(0,6\pi)} \neq 0$$

if $c_3(6\pi) \neq 0$, where $c_3(T)$ is defined by the Fourier series (46). By the perturbation theory, the kernel of $L_{\beta,\nu}$ is empty for small $\nu \in (-\nu_0, \nu_0)$.

If the linearization operator $L_{\beta,\nu}$ becomes non-invertible along the curve $\nu = \nu_S(\beta)$ of the codimension one bifurcation, the symmetry-breaking (pitchfork) bifurcation occurs at $\nu = \nu_S(\beta)$. This property gives us a criterion to find the pitchfork bifurcation numerically, in the context of the Duffing equation (69). Figure 10 (left) shows the behaviour of Floquet multipliers of equation $L_{\beta,\nu}W = 0$ with respect to parameter ν at $\beta = 0$. We can see from this picture that the pitchfork bifurcation occurs at $\nu \approx 0.00015$.

The right panel of figure 10 gives the dependence of the bifurcation value ν_S on β, for which the operator $L_{\beta,\nu_S(\beta)}$ in not invertible on $L^2_e(0, 6\pi)$. Using the formula for β in (50), we obtain

$$T = 6\pi\frac{\sqrt{1-\beta}}{\sqrt{1+2\epsilon}}.$$

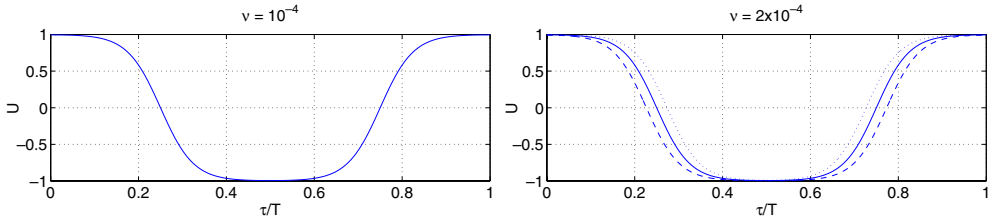

Figure 11. Solutions with period $T = 6\pi$ to equation (69) at $\beta = 0$ before (left) and after (right) the symmetry-breaking bifurcation.

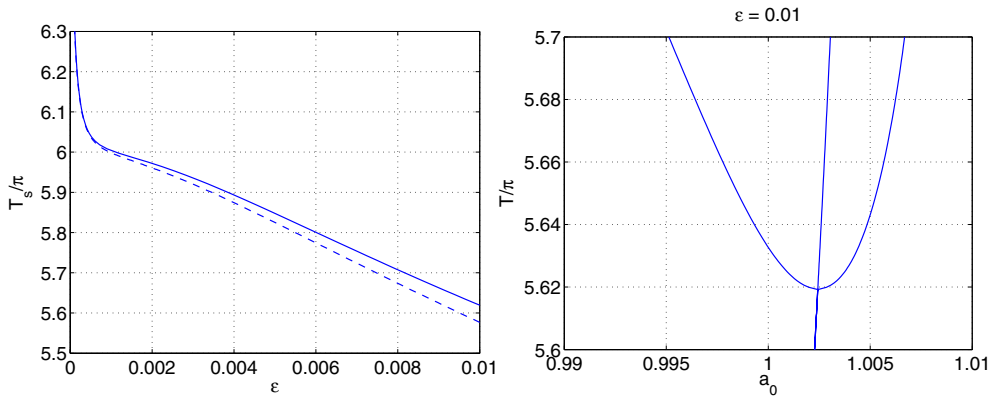

Figure 12. Left: period T_S versus ϵ at the symmetry–breaking bifurcation of the fundamental breather modelled by equation (69) (solid line) and system (42) (dashed line). Right: bifurcation diagram for the initial displacement $u_0(0) = a_0$ and period T in variables (48) computed from the 6π-periodic solution to equation (69).

As the coupling constant ϵ goes to zero, so does parameter ν. As shown in figure 10 (right), parameter β at the bifurcation curve goes to negative infinity as $\nu \to 0$. This means that the closer we get to the anti-continuum limit, the further away from 6π moves the pitchfork bifurcation period T_S. This confirms the early observation that T_S gets larger as ϵ gets smaller (see remark 5).

Figure 11 shows one solution of lemma 5 for $0 \leqslant \nu \leqslant \nu_S(\beta)$ and three solutions for $\nu > \nu_S(\beta)$, where $\beta = 0$. The new solution branches are still given by even functions but the symmetry $U(\tau) = -U(3\pi - \tau)$ is now broken. This behaviour resembles the pitchfork bifurcation shown in figure 3.

Figure 12 transfers the behaviour of figures 10 and 11 to parameters T, ϵ, and $a_0 = u_0(0)$. The dashed line on the left panel shows the dependence of period T_S at the pitchfork bifurcation versus ϵ for the full system (42). The right panel of figure 12 can be compared with the inset on the left panel of figure 2.

Remark 6. Numerical results in figures 11 and 12 indicate that the Duffing equation with a small harmonic forcing (69) allows us to capture the main features of the symmetry-breaking bifurcations in the discrete Klein–Gordon equation (42). Nevertheless, we point out that the rigorous results of lemmas 4 and 5 are obtained far from the pitchfork bifurcation, because parameter δ is assumed to be fixed independently of ϵ in these lemmas. To observe the pitchfork bifurcation in figures 11 and 12, parameter δ must be sent to $-\infty$ as ϵ reduces to zero.

Table 2. Stable two-site breathers in soft and hard potentials from [26].

	N odd	N even
Hard potential $V'(u) = u + u^3$	In-phase	Anti-phase
Soft potential $V'(u) = u - u^3$	Anti-phase In-phase	Anti-phase

6. Conclusion

We have considered existence and stability of multi-site breathers in the Klein–Gordon lattices with linear couplings between neighboring particles. We have described explicitly how the stability or instability of a multi-site breather depends on the phase difference and distance between the excited oscillators.

It is instructive to compare our results to those obtained by Yoshimura [26] for the lattices with purely anharmonic coupling:

$$\ddot{u}_n + u_n \pm u_n^k = \epsilon(u_{n+1} - u_n)^k - \epsilon(u_n - u_{n-1})^k, \tag{75}$$

where $k \geqslant 3$ is an odd integer. Table 2 summarizes the result of [26] for stable configurations of two-site breathers from the configuration

$$\boldsymbol{u}^{(0)}(t) = \sigma_j \varphi(t) \boldsymbol{e}_j + \sigma_k \varphi(t) \boldsymbol{e}_k,$$

where $N = |j - k| \geqslant 1$.

Note that the original results of [26] were obtained for finite lattices with open boundary conditions but can be extrapolated to infinite lattices, which preserve the symmetry of the multi-site breathers.

Table 2 is to be compared with table 1 summarizing our results. Note that Table I actually covers M-site breathers with equal distance N between the excited sites, whereas table 2 only gives the results in the case $M = 2$. We have identical results for hard potentials and different results for soft potentials. First, spectral stability of a two-site breather in the anharmonic potentials is independent of its period of oscillations and is solely determined by its initial configuration (table 2). This is different from the transition from stable anti-phase to stable in-phase breathers for even N in soft potentials (table 1). Second, both anti-phase and in-phase two-site breathers with odd N are stable in the anharmonic lattice. The surprising stability of in-phase breathers is explained by additional symmetries in the anharmonic potentials. The symmetries trap the unstable Floquet multipliers μ associated with in-phase breathers for odd N at the point $\mu = 1$. Once the symmetries are broken (e.g. for even N), the Floquet multipliers μ split along the real axis and the in-phase two-site breather becomes unstable in soft potentials.

We have also illustrated bifurcations of breathers near the point of $1:3$ resonance. It is important to note that a similar behaviour is observed near points of $1:k$ resonance, with k being an odd natural number. For the non-resonant periods, a breather has large amplitudes on excited sites and small amplitudes on the other sites. As we increase the breather's period approaching a resonant point $T = 2\pi k$ for odd k, the amplitudes at all sites become large, a cascade of pitchfork bifurcations occurs for these breathers, and families of these breathers deviate from the one prescribed by the anti-continuum limit. However, due to the saddle-node bifurcation, another family of breathers satisfying theorem 1 emerges for periods just above the resonance value. The period–amplitude curves, similar to those in figure 2, start to look like trees with branches at all resonant points $T = 2\pi k$ for odd k. In the anti-continuum limit, the gaps at the period–amplitude curves vanish while the points of the pitchfork bifurcations go to infinity. The period–amplitude curves turn into those for the set of uncoupled anharmonic oscillators.

Acknowledgments

The authors thank P Kevrekidis and K Yoshimura for posing the problem and stimulating discussions, which resulted in this work.

Appendix. Comparison of Floquet theory with spectral band theory and Hamiltonian averaging

We will show here that the reduction of lemma 2 for $N = 1$ agrees exactly with the main conclusions of the previous studies [2, 12] (see also [8]).

The matrix eigenvalue problem (35) for $N = 1$ can be written in the form

$$A(E)\Lambda^2 \boldsymbol{c} = \mathcal{S}\boldsymbol{c}, \qquad \boldsymbol{c} \in \mathbb{C}^M, \tag{76}$$

where

$$A(E) = -\frac{T^2(E)}{T'(E)\int_0^T \dot{\varphi}^2 \, \mathrm{d}t}. \tag{77}$$

We will show that the quantity $A(E)$ arises both in the spectral band theory used in [2] and in the Hamiltonian averaging used in [12].

For the spectral band theory [2], we consider solutions of the spectral problem

$$Lu = \lambda u, \qquad L = \partial_t^2 + V''(\varphi(t)) : H^2_{\text{per}}(0, T) \to L^2_{\text{per}}(0, T). \tag{78}$$

Let $M = \Phi(T)$ be the monodromy matrix computed from the fundamental matrix solution $\Phi(t)$ of the system

$$\frac{\mathrm{d}}{\mathrm{d}t}\Phi(t) = \begin{bmatrix} 0 & 1 \\ \lambda - V''(\varphi(t)) & 0 \end{bmatrix} \Phi(t), \tag{79}$$

subject to the initial condition $\Phi(0) = I \in \mathbb{M}^{2\times 2}$. Since $\det(M) = 1$, the Floquet multipliers μ_1 and μ_2 satisfy

$$\mu_1\mu_2 = 1, \qquad \mu_1 + \mu_2 = \operatorname{tr}(M) \equiv F(\lambda).$$

In particular, $\mu_1 = \mu_2 = 1$ if $\operatorname{tr}(M) = 2$, which is true at $\lambda = 0$ thanks to the exact solution (28),

$$\Phi(t) = \begin{bmatrix} \frac{\partial_E \varphi(t)}{a'(E)} & \frac{\dot{\varphi}(t)}{\ddot{\varphi}(0)} \\ \frac{\partial_E \dot{\varphi}(t)}{a'(E)} & \frac{\ddot{\varphi}(t)}{\ddot{\varphi}(0)} \end{bmatrix} \quad \Rightarrow \quad \Phi(T) = \begin{bmatrix} 1 & 0 \\ T'(E)[V'(a)]^2 & 1 \end{bmatrix}.$$

Hence, we have $F(0) = 2$. We will show that $A(E)$ in (77) determines the sign of $F'(0)$. Denote elements of $M = \Phi(T)$ by $M_{i,j}$ for $1 \leqslant i, j \leqslant 2$. Since $\det(M) = 1$ for all λ, we obtain

$$F'(0) = \partial_\lambda(M_{11} + M_{22})|_{\lambda=0} = M_{21}\partial_\lambda M_{12}|_{\lambda=0} = T'(E)[V'(a)]^2\partial_\lambda M_{12}|_{\lambda=0}.$$

Let $U(t)$ be a solution of

$$\ddot{U}(t) + V''(\varphi(t))U(t) = \dot{\varphi}(t), \tag{80}$$

subject to the initial condition $U(0) = \dot{U}(0) = 0$. Then, $U(T) = \partial_\lambda M_{12}|_{\lambda=0}\ddot{\varphi}(0)$. Solving the second-order equation (80), we obtain an explicit solution

$$U(t) = \dot{\varphi}(t)\left(1 - \int_0^t \dot{\varphi}(s)\partial_E\varphi(s)\,\mathrm{d}s\right) + \partial_E\varphi(t)\int_0^t \dot{\varphi}^2(s)\,\mathrm{d}s,$$

from which we find that

$$F'(0) = -T'(E)\int_0^T \dot{\varphi}^2(t)\,\mathrm{d}t = \frac{T^2(E)}{A(E)}.$$

If $T'(E) < 0$ (for the hard potentials), we have $F'(0) > 0$, which implies that the spectral band of the purely continuous spectrum of operator L in $L^2(\mathbb{R})$ is located to the left of $\lambda = 0$. If $T'(E) > 0$ (for the soft potentials), we have $F'(0) < 0$, which implies that the spectral band of L in $L^2(\mathbb{R})$ is located to the right of $\lambda = 0$. If $\lambda = \omega(k)$ is the dispersion relation of the spectral band for $k \in \left[-\frac{\pi}{T(E)}, \frac{\pi}{T(E)}\right]$, then near $\lambda = 0$, we have

$$\omega(k) = -\frac{T^2(E)}{F'(0)}k^2 + \mathcal{O}(k^4) \qquad \text{as} \quad k \to 0 \quad \Rightarrow \quad \omega''(0) = -2A(E).$$

The identity $\omega''(0) = -2A(E)$ establishes the equivalence of the matrix eigenvalue problem (76) with the spectral band theory used in [2].

For the Hamiltonian averaging [12], we consider the action variable for the nonlinear oscillator (8),

$$J = 4\int_0^{a(E)} \sqrt{2(E - V(\varphi))}\,\mathrm{d}\varphi.$$

Explicit computation shows that

$$\frac{\mathrm{d}J}{\mathrm{d}E} = 2\sqrt{2}\int_0^{a(E)} \frac{\mathrm{d}\varphi}{\sqrt{E - V(\varphi)}} = T(E).$$

If $\omega = \frac{1}{T(E)}$ is the frequency of oscillations, then

$$\frac{\mathrm{d}E}{\mathrm{d}J} = \omega(J) \quad \Rightarrow \quad \frac{\mathrm{d}^2E}{\mathrm{d}J^2} = \frac{\mathrm{d}\omega}{\mathrm{d}J} = -\frac{T'(E)}{T^3(E)} = \frac{1}{T(E)A(E)\int_0^T \dot{\varphi}^2\,\mathrm{d}t}.$$

Therefore, the signs of $A(E)$ and $E''(J)$ coincide and this establishes the equivalence of the matrix eigenvalue problem (76) with the Hamiltonian averaging used in [12].

References

[1] Ahn T, MacKay R S and Sepulchre J-A 2001 Dynamics of relative phases: generalised multibreathers *Nonlinear Dyn.* **25** 157–82

[2] Archilla J F R, Cuevas J, Sänchez-Rey B and Alvarez A 2003 Demonstration of the stability or instability of multibreathers at low coupling *Physica* D **180** 235–55

[3] Aubry S 1997 Breathers in nonlinear lattices: existence, linear stability and quantization *Physica* D **103** 201–50

[4] Bambusi D, Paleari S and Penati T 2010 Existence and continuous approximation of small amplitude breathers in 1D and 2D Klein-Gordon lattices *Appl. Anal.* **89** 1313–34

[5] Bambusi D and Penati T 2010 Continuous approximation of breathers in 1D and 2D DNLS lattices *Nonlinearity* **23** 143–57

[6] Bridges T 1990 Bifurcations of periodic solutions near a collision of eigenvalues of opposite signature *Math. Proc. Camb. Phil. Soc.* **108** 575–601

[7] Broer H, Hanssmann H, Jorba A, Villanueva J and Wagener F 2003 Normal-internal resonances in quasi-periodically forced oscillators: a conservative approach *Nonlinearity* **16** 1751–91

[8] Cuevas J, Koukouloyannis V, Kevrekidis P G and Archilla J F R 2011 Multibreather and vortex breather stability in Klein–Gordon lattices: Equivalence between two different approaches *Int. J. Bifurcation Chaos* **21** 2161–77

[9] James G, Sánchez–Rey B and Cuevas J 2009 Breathers in inhomogeneous nonlinear lattices: an analysis via center manifold reduction *Rev. Math. Phys.* **21** 1–59

[10] James G and Kastner M 2007 Bifurcations of discrete breathers in a diatomic Fermi–Pasta–Ulam chain *Nonlinearity* **20** 631–57

[11] Kato T 1995 *Perturbation Theory for Linear Operators* (Berlin: Springer)

[12] Koukouloyannis V and Kevrekidis P G 2009 On the stability of multibreathers in Klein–Gordon chains *Nonlinearity* **22** 2269–85

[13] MacKay R S 2004 Slow manifolds in *Energy Localization and Transfer* ed T Dauxois *et al* (Singapore: World Scientific) pp 149–192

[14] MacKay R S and Aubry S 1994 Proof of existence of breathers for time-reversible or Hamiltonian networks of weakly coupled oscillators *Nonlinearity* **7** 1623–43
[15] Morgante A M, Johansson M, Kopidakis G and Aubry S 2002 Standing wave instabilities in a chain of nonlinear coupled oscillators *Physica* D **162** 53–94
[16] Pelinovsky D E 2011 *Localization in Periodic Potentials: from Schrödinger Operators to the Gross–Pitaevskii Equation* (Cambridge: Cambridge University Press)
[17] Pelinovsky D E, Kevrekidis P G and Frantzeskakis D J 2005 Stability of discrete solitons in nonlinear Schrödinger lattices *Physica* D **212** 1–19
[18] Pelinovsky D E and Sakovich A 2011 Internal modes of discrete solitons near the anti-continuum limit of the dNLS equation *Physica* D **240** 265–81
[19] Sandstede B 1998 Stability of multiple-pulse solutions *Trans. Am. Math. Soc.* **350** 429–72
[20] Sandstede B, Jones C K R T and Alexander J C 1997 Existence and stability of N-pulses on optical fibers with phase-sensitive amplifiers *Physica* D **106** 167–206
[21] Simo C and Vieiro A 2009 Resonant zones, inner and outer splittings in generic and low order resonances of area preserving maps *Nonlinearity* **22** 1191–1245
[22] Simo C and Vieiro A 2011 Dynamics in chaotic zones of area preserving maps: Close to separatrix and global instability zones *Physica* D **240** 732–53
[23] Welters A 2011 On explicit recursive formulas in the spectral perturbation analysis of a Jordan block *SIAM J. Matrix Anal. Appl.* **32** 1–22
[24] Yakubovich V A and Starzhinskii V M 1975 *Linear Differential Equations With Periodic Coefficients* (New York: Wiley)
[25] Yoshimura K 2011 Existence and stability of discrete breathers in diatomic Fermi–Pasta–Ulam type lattices *Nonlinearity* **24** 293–317
[26] Yoshimura K 2012 Stability of discrete breathers in nonlinear Klein–Gordon type lattices with pure anharmonic couplings *J. Math. Phys.* **53** 102701
[27] Zeidler E 1995 *Applied Functional Analysis. Main Principles and Their Applications* (*Applied Mathematical Sciences* vol 109) (New York: Springer)